Title:
Bird-inspired robotics principles as a framework for developing smart aerospace materials

Kenneth A.W. Hoffmann[1]*, Tony G. Chen[1], Mark R Cutkosky[1], David Lentink[2]

[1]Department of Mechanical Engineering, Stanford University.
[2]Faculty of Science and Engineering, University of Groningen, The Netherlands.
*Correspondence to: khffmnn@stanford.edu

Intended for the special edition on "Multifunctional Composites for Autonomic, Adaptive and Self-Sustaining Systems.", AFOSR DESI

Abstract

Birds are notable for their ability to seamlessly transition between different locomotory functions by dynamically leveraging their shape-shifting morphology. In contrast, the performance of aerial vehicles is constrained to a narrow flight envelope. To understand which functional morphological principles enable birds to successfully adapt to complex environments on the wing, engineers have started to develop biomimetic models of bird morphing flight, perching, aerial grasping and dynamic pursuit. These studies show how avian morphological capabilities are enabled by the biomaterial properties that make up their multifunctional biomechanical structures. The hierarchical structural design includes concepts like lightweight skeletons actuated by distributed muscles that shapeshift the body, informed by embedded sensing, combined with a soft streamlined external surface composed of thousands of overlapping feathers. In aerospace engineering, these functions are best replicated by smart materials, including composites, that incorporate sensing, actuation, communication, and computation. Here we provide a review of recently developed biohybrid, biomimetic, and bioinspired robot structural design principles. To inspire integrative smart material design, we first synthesize the new principles into an aerial robot concept to translate it into its aircraft equivalent. Promising aerospace applications include multifunctional morphing wing structures composed out of smart composites with embedded sensing, artificial muscles for robotic actuation, and fast actuating compliant structures with integrated sensors. The potential benefits of developing and mass-manufacturing these materials for future aerial robots and aircraft include improving flight performance, mission scope, and environmental resilience.

1 Introduction: nature as inspiration for flight

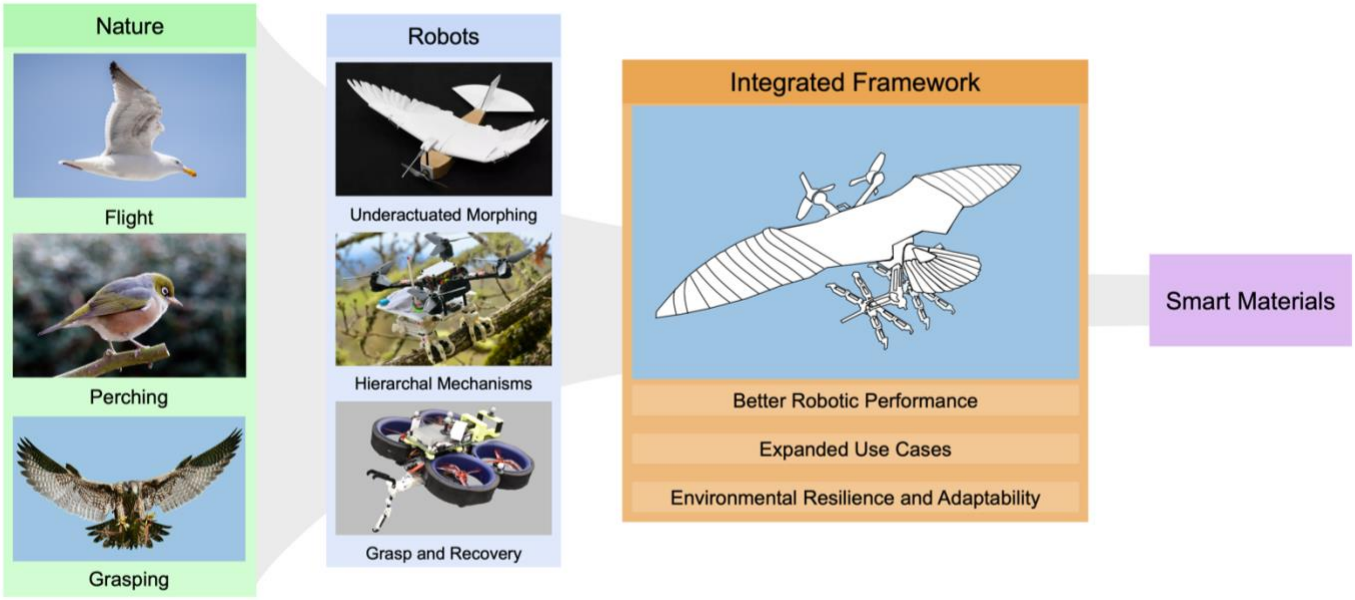

Figure 1:

Nature inspires the design of aerial robots that serve as platforms to develop new smart materials for aerospace applications. *Birds naturally perform dynamic maneuvers and react to disturbances. This ability exhibits itself across three functions: flight (photo credit World Wildlife), perching (Photo Credit Bernard Spragg), and grasping (Photo Credit Alexas Fotos). Roboticists have been inspired by these functions to develop aerial robots that mimic the capabilities by using biohybrid, biomimetic, and bioinspired structures. Three such systems ("Robots") are: A) PigeonBot (Photo Credit Eric Chang)* [1] *uses a soft robotic underactuated morphing wing comprised of real bird feathers for flight; B) The Stereotyped Nature-inspired Aerial Grasper (SNAG) (Photo Credit Will Roderick)* [2] *stores and converts energy to quickly perch or grasp; and C) The grasp and recovery robot, Aerial Grasping Robot (AGR)*[3] *can catch flying targets and quickly recover from those collisions. Combined they form an integrated framework to inspire the development of new smart and robotic materials for future aerospace applications.*

Birds are among the most advanced and highest performing flyers in nature[4–6]. The avian shape-shifting morphology, composed of biomechanical structures with tuned biomaterials, effectively integrates complex locomotory functions[6–11]. Flight, perching, grasping, and dynamic pursuit are prime examples (Figure 1, "Nature"). Birds precisely control their flight through soft, highly controllable, morphing wings and tails[6,12–14]. Flight control is informed by the sensing capabilities embedded in the body [15]. The sensing organs are found both centralized in the head and distributed over the body across the different levels of morphological organization[15]. It is not only the integrated sensing and closed-loop control that enable the avian body to perform diverse locomotor functions; additional passive design solutions also simplify control and increase robustness[16–22]. For example, during perching, birds perform controlled collisions harnessing the hierarchal biomechanical design of their legs, feet, and toes to absorb energy and achieve a secure grasp[23]. For in-flight grasping, a bird such as the peregrine falcon demonstrates its ability to plan a pursuit trajectory to collide with prey midair and then hold on to it while recovering from the impact to

continue flight[24]. These and other remarkable behaviors make birds excellent candidates for biohybrid, biomimetic, and bioinspired aerial robot design[25]. Based on efforts along these lines, recent robotics research has produced innovations in structural design, actuation, sensing, and controls approaches for aerial vehicles[1,26–29].

In this review, we show how multifunctional smart materials have the potential to integrate recently discovered and flight-tested biohybrid, biomimetic, and bird-inspired aerial robot design principles (Figure 1). Smart materials are often inspired by the form and function of biomaterials and biological structures found in nature[30]. To enable this, we first discuss the relevant biological underpinnings of bird morphology, including flight control, distributed sensing capabilities, perching, and grasping. Then, we propose to harness recent aerial robotics research that successfully uncovered—and flight-tested—key mechanistic principles that underpin avian flight. The aerial robotics findings form a lens that engineers and materials scientists can use to examine smart materials that functionally integrate sensing, actuation, communication, and computation[31]. In this work, we focus on robot designs developed by the authors of this work and place them in context of the broader research field and future opportunities. The first robotics vignette is PigeonBot (Figure 1, "Underactuated morphing"), which has soft morphing wings comprised of real feathers, making its design *biohybrid*[1]. The feathers are controlled indirectly via an underactuated system with joints providing actuation to a reduced set of degrees of freedom. We show how smart materials can potentially morph engineered wings more effectively based on embedded sensing networks that improve flight control. The second robotics vignette is SNAG, the stereotyped nature-inspired aerial grasper (Figure 1, "Hierarchical Mechanism")[2]. SNAG grasps and perches on complex surfaces using a novel *biomimetic* mechanism with a hierarchical mechanical structure. Inspired by SNAG, we review the concept of minimizing redundant structures and using artificial muscles instead of traditional actuators. The third robotics vignette, the aerial grasping robot (AGR), (Figure 1, "Grasp and Recovery"), uses a *bioinspired* compliant passive mechanism to grasp a target drone in flight and then recover from the collision disturbance[3]. Using this robot, we review how smart materials can provide additional sensing to ensure successful grasping and serve as compliant grasping structures. Finally, we present FalconBot, a new aerial robot that we developed to integrate the design principles of all three vignettes. The FalconBot concept enabled us to develop and present its aerospace equivalent and to show how biohybrid, biomimetics, and bioinspired aerial robotics can both motivate and provide a path for developing smart aerospace materials (Figure 1, "Integrated Framework"). Application of advanced future materials has the potential to increase the flight envelope, expand vehicle use cases, and enhance the environmental resilience and adaptability of large scale aerospace vehicles. As a result, we expect these new materials will also find broad use across engineering communities.

1.1 Biological context for the robot vignettes

To present the robotic vignettes within the biological context that inspired their design, we first review the avian biological system that underpins the bird flight capabilities the robots emulate. A critical feature of the system is that it integrates all levels of the organism, across molecular, cellular, organ and whole-body scales. This vast range of design scales is currently beyond the realm of engineering manufacturing; future smart materials could address this gap. These materials will need to furnish and support functions analog to key features of the avian body plan. The body is made out of biomaterials that form biomechanical structures, actuated by a tuned musculoskeletal system informed by distributed and centralized sensing processed with a sophisticated brain[15]. Specifically, we first discuss the role wing morphology plays in passive and active flight control. Then, we discuss the basic sensing modalities the bird integrates for flight control and locomotion. To understand how birds perch and grasp, we briefly discuss the latest work in understanding how birds land on a variety of surfaces. Together, these biological capabilities provide the motivation for understanding the role smart materials can play to improve the multifunctional abilities of future robotic structures. Conveniently, in every robot vignette, it was found that a subset of these integrated features was sufficient to embody the desired functions.

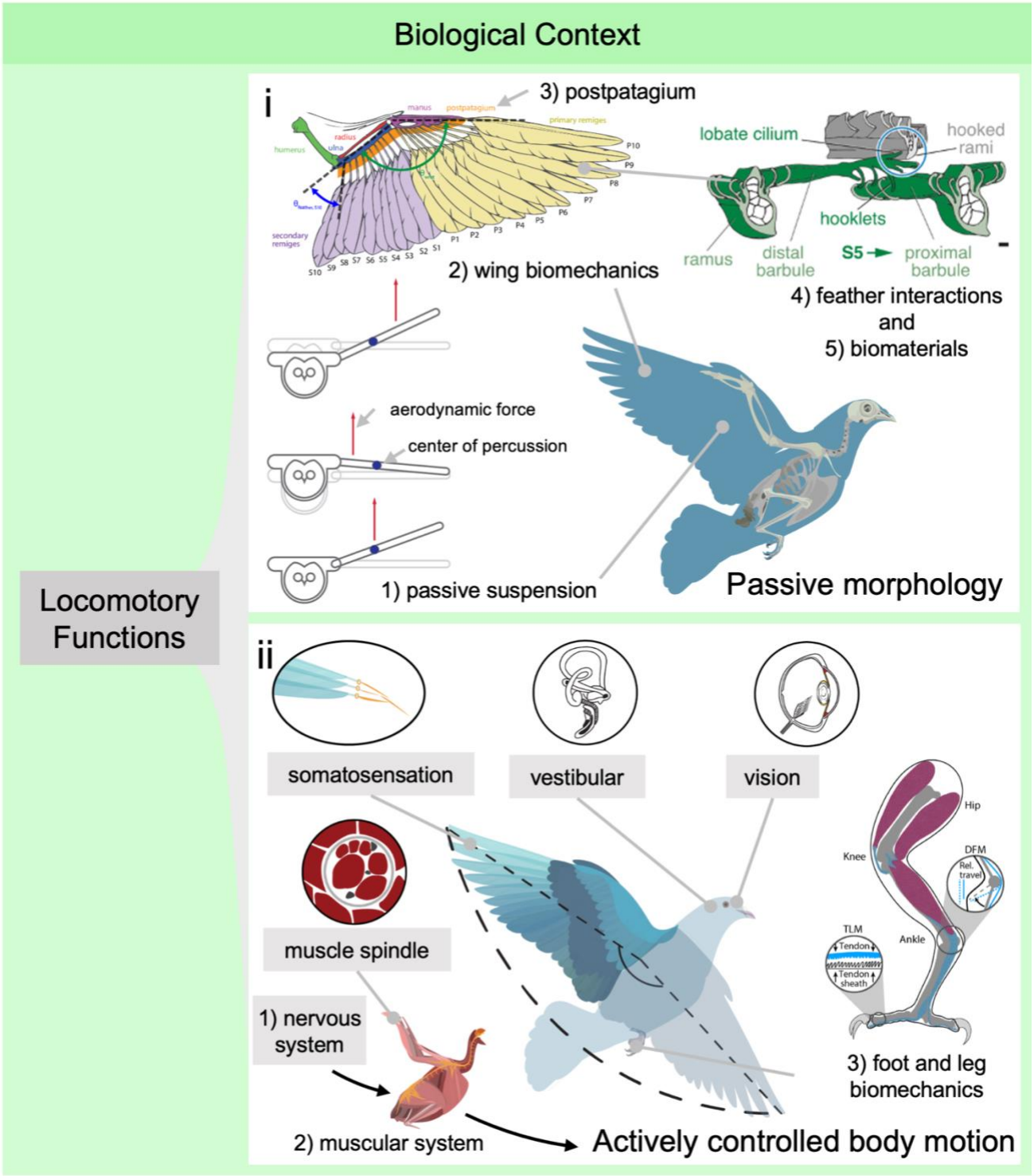

Figure 2: ***Avian locomotory functions are furnished by passively and actively controlled mechanisms. i*** *Passive morphological control mechanisms include; (1) the wing joint at the shoulder acts as passive suspension system that reduces trunk motion when gust induced forces act at the center of percussion*[19]*, (2) the wing planform and individual feathers passively deform under turbulent perturbation and thus reduce aerodynamic loading peaks further* [16,21,32,33] *(3) the elastic ligament (postpatagium) that connects all flight feathers and redistributes them automatically when the ulna and manus move* [1,12,20]*, (4) microscopic directional probabilistic fasteners lock adjacent overlapping feathers*

together (lobate cilia of underlapping feather lock onto hooked rami of overlapping feather) when they move too far apart[20]*, creating a continuous aerodynamic surface and (5) biomaterials with tailored stiffness and dampening characteristics*[21,32–34]*.* ***ii*** *Actively controlled body motion is informed by sensing organs distributed over the body (gray boxes)*[15]*. For active flight control, the bird relies on force and touch (somatosensation), vestibular, visual, and muscle spindle sensing that is communicated via the nervous system with the brain where it is integrated and translated into muscle motor commands*[15]*. Finally, when birds perch and grasp they absorbing linear and rotation energy through their hierarchical foot and leg biomechanical structures featuring a tendon locking mechanism (TLM) and digital flexor mechanism (DFM)*[23,35]*. Some of the tendons in the DFM route around the ankle which results in the toes flexing when the leg bends at the ankle*[35]*. This mechanism therefore converts the impact energy into squeezing force about the perch. The TLM acts like a ratcheting mechanism that locks the leg's posture after grasping, so the toes lock on the surface of the perch*[35–37]*. Beyond perching, this same functional principle is also used in prey-grasping to secure the prey*[37]*.*

The ability of birds to fly robustly in turbulent atmospheric flows demonstrates how effectively the avian flight control system functions[17–19,38–40]. This ability stems from the integration of both active control using sensorimotor feedback[18,38–40] and passive control based on tuned biomechanical structure properties that reduce (or eliminate) closed-loop control effort[16,19]. The key role of passive solutions to turbulent gust rejection is illustrated by how the wing's musculoskeletal system is built-up like a tuned suspension system that passively rejects gusts by enabling the wing to move with the gust to minimize trunk motion[19] (Figure 2.i.1), how wing sweep mitigates wing flutter[16], and how flexibility of the feathers lowpass filters turbulent pressure force fluctuations[9,19,41] (Figure 2.i.2). These mechanisms are based on biomechanical and biomaterial tuning across the wing's macro and microstructure that enable it to morph effectively and form a continuous aerodynamic surface with little active control input[1,20]. At the macroscale, the wing consists of feathers that shape its surface with compliant feather vanes that are each lined with a stiff rachis to form the aerodynamic load paths to the musculoskeletal system[20] (Figure 2.i.2). Along the span of the wing, the geometric properties of the vanes vary, which is thought to affect the aerodynamic forces that each vane can withstand[42,43]. The rachis of each feather is not only connected to the wing skeleton; the feathers are also embedded in and interconnected by a combination of elastic ligament and smooth muscle, known as the postpatagium tissue (Figure 2.i.3), between the base of individual feathers[44], which passively distributes overlapping flight feathers as the skeleton morphs the wing planform[20], a concept called underactuation in robotics[45]. This passive solution differs from aerospace solutions, in which closed-loop control of the motion of wing elements is a central kinematic design paradigm.

The foregoing discussion raises a question for engineers; how do bird wings morph reliably if the morphing elements are not all under closed-loop control? The relative positions of overlapping flight feathers are bounded by microstructural directionally hooked structures, which lock together probabilistically when the overlapping and underlapping directional hooking contact zones match [20]. At the microscale (Figure 2.i.4), feathers hook into each other via thousands of microscopic 3D hooks (lobate cilia) that stick out of the upper surface of the underlying feather and latch probabilistically onto 2D hooked surfaces (hooked rami) on the underside of the overlapping

feather[20]. Critically, the locking mechanism only engages when adjacent feathers spread apart too far, because that is when the hooking structure zones on the underlapping and overlapping feather match, which prevents aerodynamic gaps and helps negate turbulent perturbation[20]. The locking mechanism is also directional, meaning that whereas it resists feathers spreading too far apart—it does not resist feathers folding back together—enabling wing morphing with minimal resistance[20]. Combined with the elastic ligament, this is what enables bird wings to form a continuous aerodynamic surface with feathers. Finally, the feathers are made of a durable biomaterial, beta-keratin[46] (Figure 2.i.5).

Beta-keratin has desirable material properties, including well-tuned stiffness, strength to weight ratio, insulation, and robustness[21,46–48]. Both the material properties, and the structural organization of the feather enable them to flex while being stiff enough to avoid buckling[21,34]. Specifically, the feather's structure results in tailored flexibility along a stiff rachis lining the flexible vane, which has a relatively stiff leading edge and a flexible trailing edge[9]. Integrated, the combination of tuned material properties with a structure that is hierarchically tailored from the microscale to the macroscale enables passively dampening complex probabilistic disturbances[49]. The combination of load-bearing stiffness along the rachis with tailored flexibility along the vanes enables the feathers to bend and twist during flight, which helps alleviate the effect of turbulence intensity by passively filtering its frequency spectrum[33,50]. The described passive mechanisms supplement active control, and not all disturbances can be sufficiently filtered by the tuned structure[17,51].

Larger perturbations require active control for stable flight (Figure 2, "actively controlled body motion")[38,41]. In turbulence, small flyers, like hummingbirds, compensate by adapting the shape of the wing and the frequency of the wing stroke[38] . Changing the shape and orientation of the wings and tail as well as how the wings beat enables birds to mitigate the perturbing aerodynamic forces acting on their body. They control their bodies response to perturbations through musculoskeletal actuation of their wings, tails, trunk, legs, and feet (Figure 2, "neuromuscular system")[52–54]. Musculoskeletal motion is controlled by the central nervous system, the brain and spinal chord of the bird, which integrates high bandwidth external and internal state information sensed by centralized organs in the head as well as sensory modalities distributed over the body to inform its control policy[15,17] (Figure 2.ii, "Nervous System"). The main forms of centralized sensing that the bird harnesses for flight control are vestibular sensing, of linear and angular head motion as well as the direction of gravity, and visual sensing, of the scene surrounding the bird, which are both located in the head (other forms of centralized sensing include air speed as well as navigation cues that we do not review here). Key forms of distributed sensing include somatosensation, to sense feather loading and vibration, and muscular spindle sensing, to sense muscle stretch, the latter is critical for musculoskeletal control[15].

Centralized and distributed sensory information are integrated in the brain to inform body motion control. At the wingbeat kinematic scale, innervated feathers detect local force magnitude and

oscillation such as those resulting from stall, flow separation, and airspeed[15,55]. Beyond external flow condition, muscle spindle sensing can monitor internal joint angles as well as muscular and tendon length changes[55,56]. Supplemented by vestibular sensing, the bird achieves attitude control, reflexive control, and posture control with head-body stabilization. The bird head is stabilized in 3D by the neck along all six degrees of freedom except forward motion[22], informed by both vestibular and neck muscle spindle sensing[57]. Head stabilization and orientation control enables both the vestibular and visual system to perform better, and the brain to actively direct its perception. Stabilization of the eyes is critical for visual sensing, resulting in unblurred vision, which is important for reliable optical flow-based flight stabilization, trajectory control, and obstacle avoidance[15,58]. Integrating these sensing modalities, birds inform their biological control to achieve their diverse locomotory functions (Figure 2, "Locomotory Functions")[59].

Striking avian locomotory functions include how birds use their legs and feet in flight. Birds land and takeoff from complex surfaces while also accommodating for environmental factors such as wind gusts or minimal visual information[22,23]. This is demonstrated by the challenge of perching on diverse surfaces, which involves (i) identifying suitable perching sites and approaching them with a stereotypical trajectory[60,61] and (ii) establishing a firm grip upon landing[23,35,62]. The first of these challenges is addressed by integrated-sensing informed body motion control as noted previously. The second is addressed by the leg's biomechanics upon landing, during which the bird absorbs kinetic energy and stabilizes its grasp around a perch (Figure 2, "foot and leg biomechanics")[23]. This was quantified through parrotlet landing experiments on an instrumented perch that show that they accomplish a secure grasp on complex surfaces by combining predictable toe pad friction with probabilistic friction from their claws latching onto surface asperities[23]. Specifically, they first conform to the perch and then drag their claws over the surface to find asperities that furnish the secure grasp. This is essential for absorbing the high loads of the controlled collision birds make with the perch to land. Key elements to this automated perching mechanism (APM) are the Tendon Locking Mechanism (TLM) and the Digital Flexor Mechanism (DFM)[23,35]. First the tendons of the DFM route around the ankle such that the toes flex automatically when the leg bends at the ankle to absorb the controlled collision with the perch [35]. This mechanism converts the impact energy into elevated perch squeezing force. Then, when the legs collapsed sufficiently to absorb the collision and the feet grasp the perch securely, the TLM acts like a ratcheting mechanism that locks the legs and feet tendons so the toes lock on the surface of the perch securely, while minimizing active muscle tensioning[35–37].

An important principle that emerges from the biological context is that birds harness their biomechanical structure and mechanisms for multiple purposes to furnish an unusually broad operational envelope—as compared to robotics and aerospace design. For example, a bird uses its legs and feet for locomotion, manipulation, perching, and grasping[63–66]. Looking ahead to other functions, perching is analogous to dynamic aerial grasping (to catch an object on the wing) in that the bird needs to absorb a significant controlled aerial collision with their legs while closing their

feet and claws around an object[2]. This illustrates how birds use a single biomechanical structure for a wide range of tasks that have no engineering analog. Overall, the diverse locomotory functions of birds are the result of multifunctional integration across their bodies hierarchical levels of organization. Understanding the avian body's basic biological functions in the context of flight is essential to understand how flight-tested biohybrid, biomimetic and bioinspired aerial robots based on these biological principles can accelerate the development of smart materials for aerospace applications.

2 Flight Biohybrid robotics vignette 1: PigeonBot's underactuated morphing wings with soft bird feathers

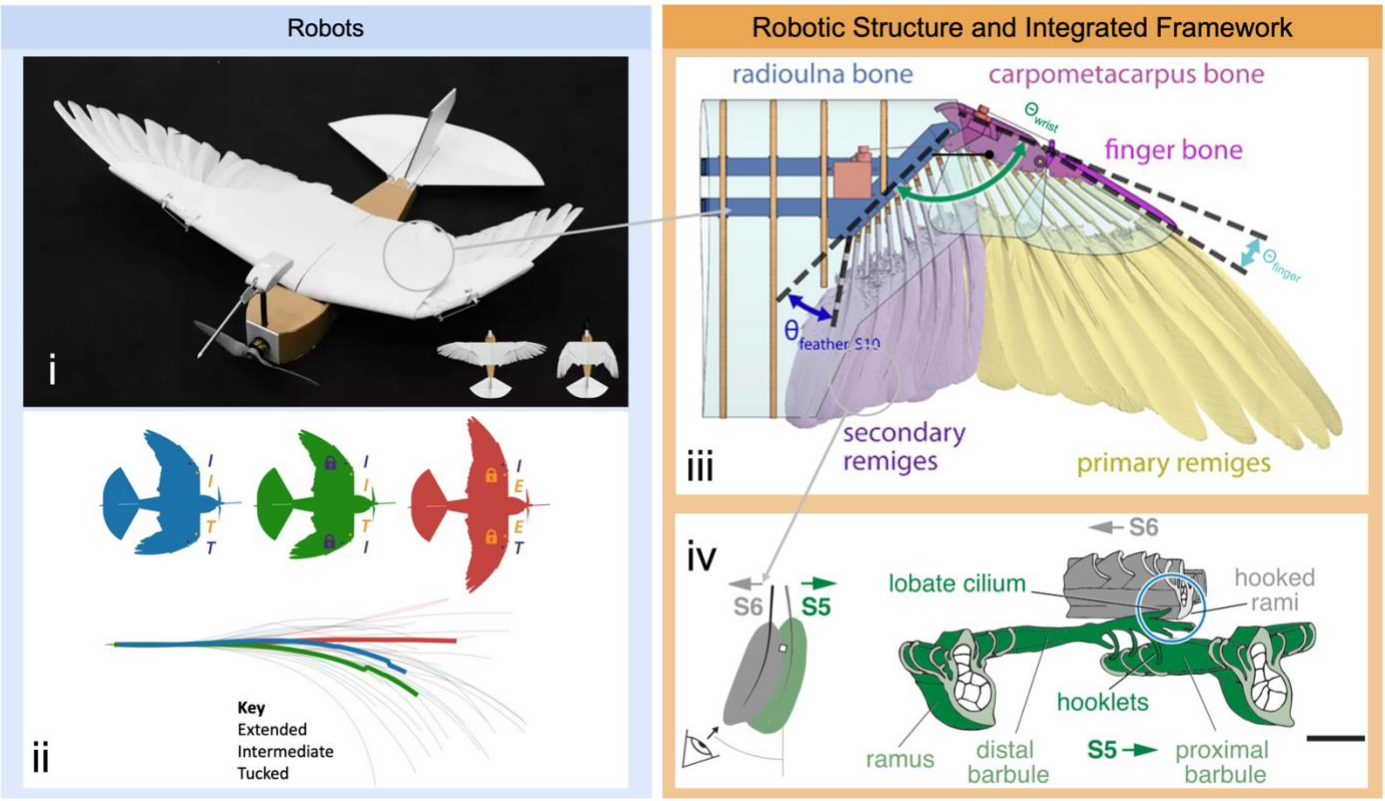

Figure 3:

PigeonBot uses an underactuated soft robotic wing with real feathers from a pigeon to stably control its flight [1]. ***(i)*** *An overview of the aerial robot that demonstrates the ability to morph by changing the planform's shape. The two small images in the bottom right show the extension and flexion range of the morphing wing.* ***(ii)*** *A subset of the curved trajectories initiated through asymmetrical wing morphing, showing the robot can turn by morphing one wing half more than the other.* ***(iii)*** *A CAD model of the morphing wing design shows how real bird secondary and primary flight feathers are integrated in the biohybrid design. The feathers are mounted on feather holders that are connect via a pin joint with the 3D printed bone structure. The bone structure features a servo-actuated wrist and finger joint that form biomimetic robot arms. The feathers are connected by tuned elastic bands (not shown) that mimic the avian elastic ligament that automatically coordinates feather motion when the robot arms move. The ability of feathers to overlap smoothly stems from their graded softness and enables the robot to morph continuously in flight.* ***(iv)*** *Adjacent flight feathers have contact zones that match and lock together probabilistically when feathers spread apart too far, and unlock again automatically when they fold together again, making the fastening mechanism directional* [20]. *The upper surface of the underlapping feather has thousands of 3D hooked lobate cilia (of about ten micron size) that latch onto the 2D hooked rami that stick out from the lower surface of the overlapping feather* [20].

PigeonBot (Figure 3, i) flies with a soft biohybrid morphing wing (Figure 3, iii). The wing features a lightweight, 3D printed, skeletal structure actuated by servos, which underactuate an array of real flight feathers via connective elastic elements (tuned elastic bands) that shape the smooth aerodynamic surface[1]. By changing the shape of its wing asymmetrically, PigeonBot can fly through a range of curved trajectories (Figure 3, ii). Each side of the wing (Figure 3, iii) can morph independently based on wrist and finger motion, causing a lift force differential between the left

and right sides of the robot[1]. As a result, a net aerodynamic torque is exerted on the robot body that induces turning motion. This enables PigeonBot to control turns of varying curvature using variable asymmetric wing morphing controlled by servo inputs to its two wrist and two finger joints, without using its rudder (Figure 3, ii)[1]. As the servo actuated skeleton extends and flexes the 3D printed wing skeleton, biomimetic robotic arms, the flight feather array expands and contracts automatically[1]. PigeonBot's flight feathers are interconnected at the base by tuned orthodontic elastic bands, which mimic how the avian elastic tissue and smooth muscle of the patagium (Section 1.1) redistributes feathers passively when the skeleton moves (Figure 3, iii)[1,20]. PigeonBot uses pigeon flight feathers because of two essential hierarchal structural properties that cannot be replicated with 3D printing at present[67]. The first is that flight feathers have a hierarchically designed structure that make them both stiff enough along the rachis to carry aerodynamic load and soft enough along the vanes to slide smoothly over each other, while also being extremely lightweight. The second is that overlapping flight feathers have specialized interaction zones with microscopic directional probabilistic fasteners that automatically lock adjacent feathers together (Figure 3, iv) before they are elastically redistributed too far apart during unfolding—preventing aerodynamic gaps—the same mechanism automatically unlocks the feathers again during wing folding[1,20]. In summary, the unique elastic feather distribution and directional probabilistic fastening mechanism together enable the avian wing to fold and unfold continuously without controlling the feather positions directly[20]. This is called "under actuation" in robotics and greatly reduces the number of servos, sensors and control loops needed for the many degrees of freedom in the wing, the position of 40 feathers is controlled by only four servo motors. Remarkably, the position control of each of the 40 feathers via the elastic ligament is highly repeatable and accurate during dynamic morphing. This high kinematic performance stems from the high natural frequency of the feather underactuation system, which is ten times higher than the servo actuation frequency bandwidth. This ensures the feather-position transfer function is governed by the linear elasticity of the elastic bands (feather mass is extremely low and surface friction is insignificant). The high kinematic performance of elastic underactuation (tested in high turbulence and flight) shows the aerospace design paradigm in which each degree-of-freedom must remain under closed-loop control can be dropped in favor of a simpler biomimetic design paradigm[1,20].

2.1 Smart materials for soft robotic wings

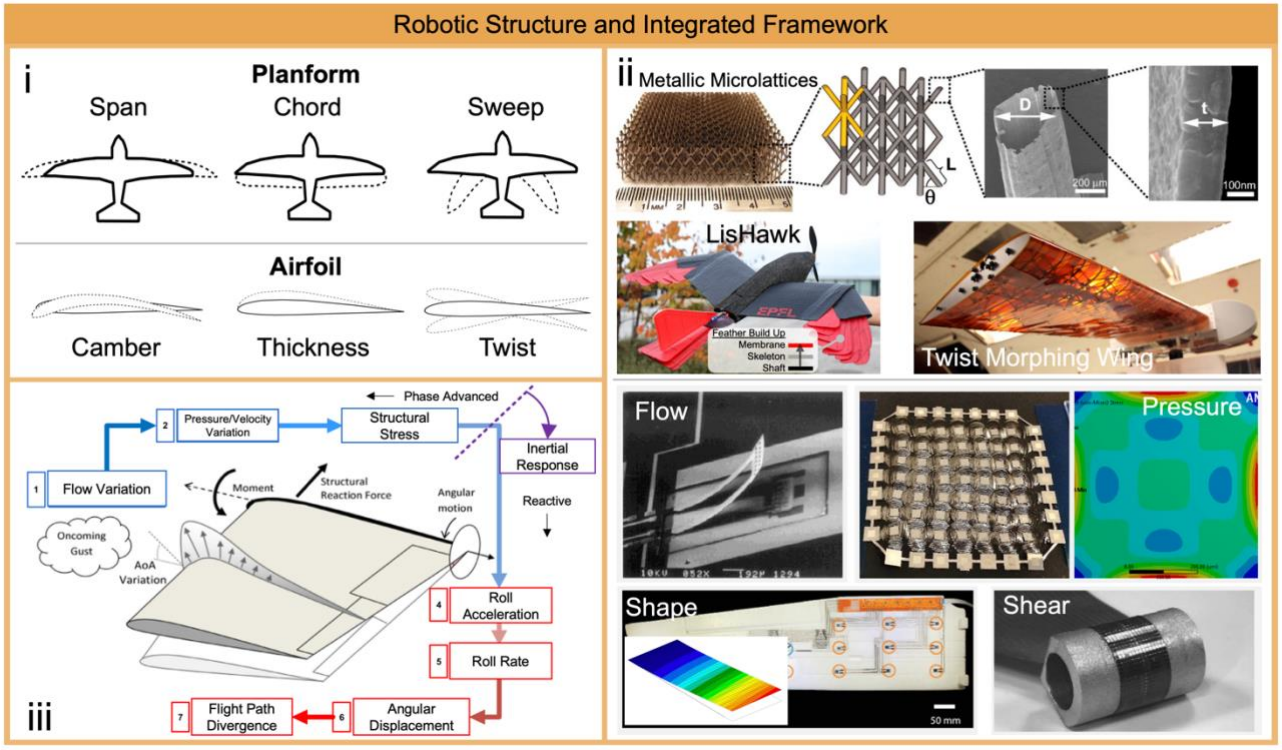

Figure 4:

Morphing wings with embedded actuation and sensing can improve flight performance, control, and environmental resilience. (i) *The two main categories of wing morphing are airfoil and planform morphing*[68]*. In airfoil morphing, the shape of the airfoil changes in the plane, in planform morphing the overall shape of the wing changes*[68]*.* ***(ii)*** *New materials for wing morphing include embedded actuation and hierarchical materials that replicate the behavior of biomaterials. Smart materials are relevant at both the wing structure level as well as the wing material level. The "twist morphing wing" uses structures with different material and structural stiffnesses to demonstrate active continuous wing twisting*[69]*[Photo Credit Kenneth Cheung/NASA]. LisHawk*[26] *flies with morphing wings and tails buildup by artificial feathers. Metallic micro-lattices are one promising hierarchical material which could be used to develop new wing structures and surfaces*[70]*. The bottom half of the panel shows different types of embedded wing sensors, including flow*[71]*, pressure* [72]*, shape* [73,74]*, and shear*[75] *sensing. Pressure and shear sensing enable fly-by-feel, which is based on wrench (force and torque feedback) control to improve flight performance. Shape sensing could be used in vision based autonomous aerial robots for active camera calibration. Shear, pressure and flow sensing can be used to detect flow separation and laminar-turbulent boundary layer transiton to optimize wing aerodynamics.* ***(iii)*** *Traditional aerial robots have IMUs embedded that are reactive sensors that measure changes in magnetic heading, angular rates and linear acceleration*[76]*. Phase-advanced sensors measure or predict a disturbance before an inertial response. Embedded sensing in the wings enables an aerial robot to respond to aerodynamic disturbances and compensate for them in advance of the inertial response of the whole vehicle.*

Drawing inspiration from birds and biohybrid robotics, smart materials can be developed to embed morphing wing principles directly in material properties together with distributed sensing to inform more advanced control. To show how smart materials could embed the morphing wing principles put forward by robot vignette 1, we focus on two main applications of smart materials (Figure 4). The first application is the use of artificial composite feathers and actuated materials

to form smart morphing wing and control surfaces (section 2.2). The second application makes the morphing wing and control surfaces smart by embedding sensor networks that sense aerodynamic, structural, and dynamic loading distributions as well as wing shape deformation to inform autonomous flight control (section 2.3).

2.2 Composites for wing and control surfaces using artificial feathers and actuated materials.

PigeonBot uses real pigeon feathers, which are not scalable beyond bird dimensions. Therefore, we need smart structures and materials that replicate the morphing functions that stem from feather structural hierarchy including graded stiffness/softness and microscopic directional probabilistic fastening. One of the first aerial robots that morphed with artificial feathers was the RoboSwift, which features eight carbon fiber feathers that slide over each other[77]. A weakness of this design is that the number of feathers is low and they lack graded stiffness. A more recent robot, the LisHawk (Figure 4.ii, "LisHawk")[78], features 18 total (9 per wing) artificial feathers that are layered to form a continuous surface. Each feather has a graded stiffness and is built up as follows (Figure 4.ii. "Feather Build Up"): a stiff central rachis, made of carbon fiber, is affixed to a glass fiber skeleton. The rachis and glass fiber assembly is then lined with a ripstop fabric polyester membrane[78]., The resulting assembly is a low mass structure that is stiff along the feather length axis, to absorb the aerodynamic forces during flight, and soft along the width axis to enable the feathers to more smoothly slide over each other. While effective, the artificial feathers in LisHawk are still heavy compared to bird feathers as well as delicate and difficult to manufacture at scale[78]. There is a need for engineering composites innovations that can provide the benefits of real feathers while being suited to high volume production[67]. We envision new, feather-inspired, cellular composites with graded stiffness to enable continuous morphing at the materials level[68,79]. The elastic connectivity between feathers can be reimagined as graded stiffness distributions in the material with a much more extreme stiffness range over many orders of magnitude than traditionally considered. Further, complex servo-actuated skeletal mechanisms could be replaced by distributed local actuation embedded in the morphing material.

Smart materials could use the same hierarchical architectural elements as feathers (section 1.1) to improve robotic wings by creating stiff, yet soft, aerodynamic wing and control surfaces[80]. An example of an ultralight material that could be used to improve aerial robot wings are ultralight microlattices (Figure 4.ii, "Metallic Microlattice")[70]. These lattices use a hierarchical structure to achieve superior material properties relative to conventional implementations of the same base materials[70]. Like feathers (section 1.1), each level of the hierarchy contributes to the overall behavior of the material. The benefits of an organized hierarchy (as compared to an unordered structure like a foamed plastic or a single level of organization as found in traditional composite layups) are consistent across different categories of materials. For example, polymers[81] and fibrous materials[82] both benefit from similar hierarchical design approaches as well, so there are several

base material candidates for new artificial feather-inspired hierarchically structured materials. Further, different base materials could be combined to achieve the desired graded stiffness of the real feather counterpart. New multi-material 3D printing based production techniques have the potential to produce these engineered materials in high volume with tight tolerances[79]. The microarchitectural approach of the materials described in this section could also lend itself to designing microscale interactions like the probabilistic directional fastening of the natural feather counterpart.

The probabilistic nature of hooking elements can also be translated to smart materials to develop new fasteners. Probabilistic mechanical fasteners are comprised of one or two surfaces with many hooking elements, where only a subset of the hooking elements engage. Though not all of the elements engage, the fasteners are still effective because the rely on the interactions of only a percentage of the hooking elements[67]. Currently, no equivalent biological or technological fastener exists that can replicate the directional probabilistic locking and unlocking of flight feathers[67]. Such directional probabilistic fasteners are useful because they provide a strong, versatile, repeatable connection without the need for precise alignment for mating between components[67], thereby reducing computation, sensing, and actuation requirements. As a result, newly developed fasteners based on smart materials that mimic feather directional probabilistic fastening could generally furnish the microstructural interactions necessary for soft robotic continuous morphing surfaces.

Material design for morphing wings

Birds actuate their feathered morphing with their forelimb musculoskeletal system, which shape-shifts the soft aerodynamic surfaces[25,83]. This morphology results in an aerodynamic surface with high levels of actuation and adaptability. Replicating the underpinning design principles in robotic morphing wings is a key step towards achieving bird-level robustness and adaptability, which exceeds current robot performance[25]. One of the challenges in this is that unlike birds, robots typically use rigid wing structures because shape-shifting wing structures are not easily replicated by engineered designs[25]. In contrast, current aerospace wing designs are discontinuous – using discrete stiff elements like slats, flaps, and ailerons to change the shape of the similarly stiff wing [84]. A consequence of this is that airplane wing airfoils can only be optimized over a few stages of flight[68] and cannot reject turbulent gusts effectively. To optimize for more stages of flight, engineers have developed methods to dynamically change the shape of the wing[68]. This requires entirely new wing designs and replacing traditional actuation methods with actively morphing wing structures and surfaces.

Morphing wing designs fall into two main categories, planform and airfoil morphing (Figure 4.i)[68]. The planform subcategories include span, chord, and sweep morphing whereas the airfoil subcategories are camber, thickness, and twist morphing[68]. By changing the shape in flight, the goal of morphing wings is to replicate the wing kinematic and shape degrees-of-freedom of birds

and therefore optimize wing shape and kinematics across the entire flight envelope[68]. Due to the complex shape and actuation requirements, the adoption of morphing wings is nearly entirely limited to experimental research platforms, but new materials could enable broader application[68]. While a few notable examples exist, such as the F-14 and the Wright Flyer, the overall lack of implementation is partially because it is difficult to design simple, reliable, and easy to fabricate (and maintain) mechanisms and structures that accomplish smooth, continuous wing morphing. An example of this challenge is shown through computationally designing a mechanism that replicates pigeon wing kinematics[85]. Six-bar mechanisms are necessary to accurately approximate the complex morphing motion of the pigeon wing, because four-bar linkages fitted to bird data lock or result in infeasible biological configurations that have engineering disadvantages[85]. This finding shows the challenge in replicating true bird wing morphing kinematics and suggests the need for different engineering approaches beyond traditional mechanism design. A solution to this challenge is to integrate distributed actuation in a structure with tunable stiffness such that implements multiple categories of wing morphing directly via smart material design.

Smart materials with tunable stiffness and embedded actuation are poised to more simply replicate the functions of soft morphing bird wings and thus have the potential to translate bird morphing wing principles to large-scale aerospace applications[68]. An example of tunable wing design is demonstrated by a cellular twist morphing wing (Figure 4.ii, "Twist Morphing Wing") that is actively deformable through variable stiffness along the wingspan[69]. The wing is constructed with modular base elements that build up to form a cellular composite structure[69]. This design approach enables spatially tuned stiffness by varying the material choice and geometry of a specific cell in the overall assembly[69]. As a result, local stiffness can be calibrated to produce the desired wing morphing behavior[69]. While we envision wings morphing as a whole, applying the principles to smaller sections of a wing can improve the flight efficiency of intermediate designs. In this case, smart materials could be used to control small sections of a wing (like active winglets and continuously twisting flaps)[86–91]. Whether by enabling global or local morphing, smart materials promise better performance as compared to traditional discrete airfoil modification strategies, over a wider range of flight conditions[68]. Future morphing wings could combine this tuned stiffness approach with distributed actuation and control informed by distributed sensing networks. Morphing wings present new opportunities and challenges for distributed sensing and control algorithms to improve flight performance. In the following section, we describe how smart materials can enable the control of morphing wings informed by distributed local sensing of airflow conditions[92].

Scaling Principles for Morphing Wing Design

Two key design principles emerge to scale morphing wings. First, the wing surface must be capable of elastic redistribution with a stable quasi-static response to control input[1]. In the case of PigeonBot this requires that the natural frequency of the ligaments connecting the aerodynamic morphing elements must be an order of magnitude higher (10 times) than the actuation frequency[1].

As a result, the wing morphing action can be considered quasistatic because the static effects dominate the dynamic effects of the morphing wing movement[1]. Additionally, this is thought to help avoid flutter in the individual wing elements[1].

The next consideration for scaling morphing wings is preventing aerodynamic gaps through directional fasteners that scale[20]. While the aerodynamic force on the wing increases with wing area, the number of directional hooking fasteners of feathers also scale directly with wing area. As a result, as wing area increases, the number of fasteners should increase at the same rate, meaning that the hooking force also increases with wing area. Therefore, the velcro-like hooks of the feathers continue to provide sufficient directional fastening force to prevent aerodynamic gaps as the wing size increases. Considering a similar design principle into new morphing wing material design will be important to ensure continuous morphing and smooth, gap-less aerodynamic surfaces.

These two scaling principles should be considered in the design of future smart materials to ensure controllable wing morphing behavior with predictable response.

2.3 Embedded sensing in wing structures for bioinspired flight control and autonomy

Aerodynamic sensing for better flight control

PigeonBot, like most aerial robots, relies on four main sensing modalities for state estimation. These include an inertial measurement unit (IMU) (containing an accelerometer, gyroscope, and magnetometer), a GPS for position, a barometer for pressure sensing, and a pitot tube for airspeed estimation based on the dynamic pressure differential[93]. The sensors fall into two categories: phase-advanced and reactive (Figure 4.iii)[94]. Phase-advanced sensors detect or predict disturbances before an inertial response[76,94]. Most of the sensors used for flight control today are reactive, detecting or estimating inertial responses[94]. Smart materials could enable better integration of phase-advanced sensing into robotic morphing wing and tail structures by measuring aerodynamic and structural quantities directly, like the distributed sensors of the bird (section 1.1).

Aerial robots and aerospace vehicles generally– particularly those with compliant structures – would benefit from bird-inspired surface and structural sensing, leading to new predictive control schemes[95] that compensate for disturbances before they produce large inertial effects that accumulate to result in significant deviations from the intended flight trajectory[76,94]. To implement this control scheme, the robotic structure will need to be able to sense aerodynamic properties or structural stresses using phase-advanced sensors[95]. Through material development focused on incorporating such sensors into robotic structures, we envision further improvement to sensor networks integrated at the time of manufacturing, rather than as discrete elements added to, or layered on, existing structures.

Sensing skins are a recent development that add sensing to a surface or structure, with the added potential to be integrated into a robotic structure during manufacturing[96]. To sense aerodynamic and structural properties, sensing skins typically use shape, pressure, airflow, and shear sensing, though broader sensing capabilities could also be incorporated. (Figure 4.ii, bottom half) [96]. Shape sensing using strain measurements is useful to determine wing displacement, accelerations, torques, and changes in structural loading[74,96]. Pressure sensing is useful for determining the aerodynamic characteristics of the vehicle's external surfaces[76,95,97] (wing, tail, etc.) including aerodynamic load[72,98–100], atmospheric turbulence intensity[97,101], laminar-turbulence transition in the boundary layer flow[102–105], and the lift and drag distributions[99,104,106]. Near-surface flow sensing enables detection of flow separation from the surface[107,108]. Similarly, shear sensing can be used to further monitor laminar-turbulent boundary layer transition and flow separation[75,109–111]. These examples show that, as in Kalman filtering, the fusion of multiple sensory modalities have the potential to greatly reduce the uncertainty in online vehicle state estimation[112]. Here, we present isolated examples of embedded sensor applications because those dominate the literature (the IMU in autonomous vehicles is a key exception, but it's centralized). To leverage the full potential of these different sensing modalities, they should be fused algorithmically in future applications, because combined they provide more continuous and reliable state information about the wing structure and airflow.

To illustrate key components for future integrated aerospace sensing skins, we focus on specific sensor solutions for estimating structure and flow parameters. To measure wing shape, a soft skin with embedded strain sensors adhered to a wing surface can predict the shape of the wings of a small, fixed-wing robot[74] (Figure 3.ii, "Shape", background). Beyond strain gauges, fiber optics have also been used for similar measurements (Figure 4.ii, "Shape", foreground)[73]. Based on strain and shape measurements, changes in flight dynamics of the aerial robot can be inferred, paving the way towards using this information for control. Moving beyond structural properties, flow can be measured with a piezoresistive mass flow MEMS sensor[71] (Figure 4.ii "Flow"). This sensor uses little power and is adaptable to a variety of flow conditions by slightly changing the shape of the sensor[71]. Multiple form factors of these small sensors could be placed along the wing surface to measure the flow to determine flow direction and magnitude[71]. Calibration challenges may arise under variable operating conditions, which can be mitigated by incorporating additional sensing of pressure and temperature[71]. To measure pressure, an expandable network of sensors connected by stretchable polyimide wires (Figure 4.ii, "Pressure") can perceive distributed pressure over a surface[72,113,114]. The low thickness profile of this sensor network makes it possible to embed it into wing (and other) surfaces[114]. Because pressure and flow together do not tell the full story of the conditions across the wing surface, shear sensing is also useful for detecting flow separation at critical points of the wing. A flexible sensor skin measuring surface shear stress (Figure 4.ii, "Shear")[75] is an early example of using a shear sensor to detect flow separation along the leading edge of an airfoil, and therefore can be used to predict stall. The data from sensing skins should

be fused to paint a complete picture of the aerodynamic and structural properties of the wing to inform vehicle state monitoring and autonomous flight control.

Control schemes that use structures with embedded sensing for flight control are colloquially known as "Fly by Feel"[113,115]. These control schemes rely on phase-advanced sensors and therefore respond directly to aerodynamic and structural disturbances, (Figure 3.iii)[94]. Examples of "Fly by Feel' include rotorcraft that use strain sensors embedded in the robot frame to reject disturbances[116] or the control of a vertical (VTOL) concept aerial robot that compensates for wind during the transition from hover to forward flight[117]. This robot uses a 3D airflow sensor to detect aerodynamic forces but would benefit from using an integrated sensing skin instead for improved situational awareness. Overall, structures incorporating sensing skins have the potential to streamline the design of these example aerial robots by integrating the sensors directly into the material of the airframe's structural elements like how flexible printed circuit boards (PCBs) are assembled, thereby reducing the need for current unwieldy manual aerodynamic flow or strain measuring device assemblies. The benefits of integrating sensing into a wing structure extend beyond flight control and could improve autonomous systems broadly by assisting in-flight calibration of multiple embedded navigation cameras.

Current fully autonomous robots, in particular small quadcopters, use vision for localization through 360 degree visual inertial odometry (VIO) based on multiple embedded cameras[118–121]. Like the motor arms of quadcopters, the wings of an aerial robot are an ideal location to mechanically integrate cameras for 360 degree stereo localization, however a challenge with autonomous vision-based aerial robots is constant online camera calibration and system failures stemming from poor calibration[122]. The long baseline and unobstructed field of view that multiple cameras mounted on a wing offer are advantageous, but the deflections and aeroelastic vibrations of wings represent a problem. This is not only the case for soft and bioinspired wings of small robots, it's a much more significant and hard problem for large, unmanned vehicles and full-scale aircraft, because the square-cube scaling law makes their wings disproportionally flexible. Instrumenting these wings to monitor structural deflections phase-advanced in real-time is essential to compensate for the associated camera motion robustly beyond what a purely algorithmic solution may offer.

Demonstrations of embedded wing sensing for attitude (vehicle state) estimation or flight control remain confined to laboratory and research projects – for example, in wind tunnel tests[123]. Scaling challenges stemming from hardware and software are one barrier to broad implementation of sensing skins[96,123]. These hardware challenges including sensor capability, the density needed for accurate distributed sensing and integration during fabrication[96,123] are among the most difficult aspects of implementing sensing skins. New manufacturing techniques can address hardware challenges through sensor installation at time of fabrication[96]. For example, the advancement of 3D printing technologies will play a role in future sensing skins by making it easier to integrate

electromechanical components into a wider array of materials[124]. Additional challenges arising from the number of wires, interconnects, and bandwidth can be solved by wireless sensor networks with distributed data processing[125]. Further software challenges include modeling and computation[96,123]. Surfaces with complex geometries will need more accurate simulation and modelling to isolate material behavior from sensor outputs.

Designing sensing skins for new trends in vehicle design, including bioinspired morphing surfaces, are a particular challenge[126]. A short-term solution is to develop the sensor networks as small patches in static areas where aerodynamic conditions are of particular interest[127]. A better, long-term solution is embedding the sensorized morphing skins in smart actuated materials so that the effect of changing shape is compensated for in the sensor outputs[96,126]. Finally, advances in sensing skins are driven by other applications areas including ongoing development of robots that are safe for human interaction[128]. Therefore, collaboration among the different application communities can advance the development of practical sensing skins across requirements.

3 Perching Biomimetic robotics vignette 2: SNAG's stereotyped nature inspired aerial grasper for perching

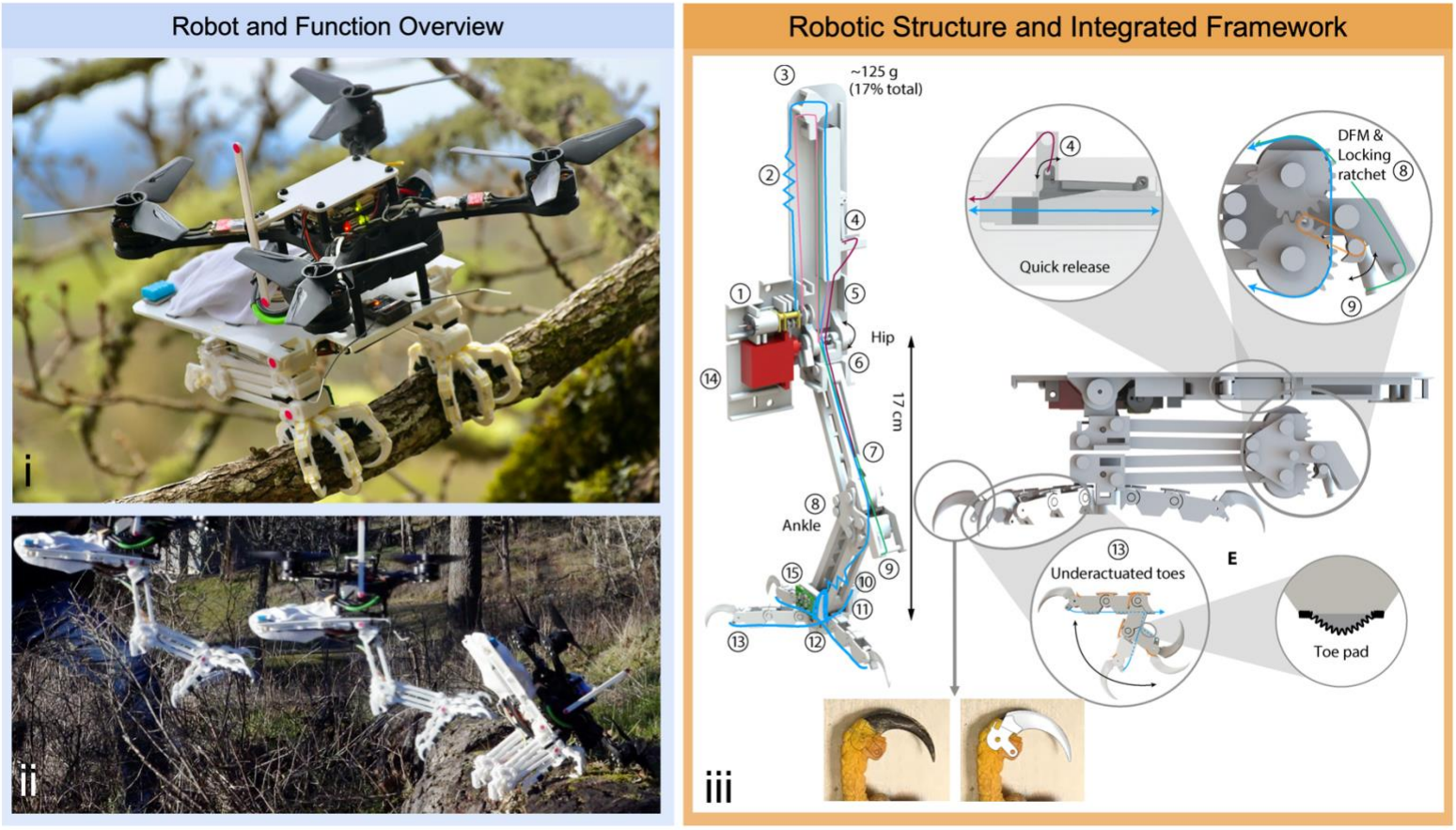

Figure 5:

SNAG is a robotic leg and end effector that mimics bird legs and feet; its biomimetic mechanism design enables takeoff and landing on complex surfaces. (i) *A quadcopter perched on a branch with SNAG.* ***(ii)*** *SNAG's dynamic landing sequence.* ***(iii)*** *The right panel demonstrates the hierarchical structure of the mechanism. This mechanism enables SNAG to collide with the branch, absorb the impact energy, and stabilize on the perch. The structure (predominantly) and claws are made of 3D printed PLA. To mimic the toe structure of a bird, each phalanx of SNAG's feet features a deformable rubber pad covered with grip tape to add surface waviness for locking onto surface irregularities. The claws latch onto stochastic surface asperities of the branch with elevated force that together with reliable, but lower, toe pad friction forces help absorb the angular momentum during collision and provide the torque needed to perch when the center of mass is off center.* [2]

The stereotyped nature-inspired aerial grasper (SNAG)[2] is a biomimetic perching mechanism based on recent findings[23,66] in birds' ability to grasp and perch on unstructured surfaces. SNAG combines active and passive controls to land on a range of perches by absorbing the impact energy through its two-leg mechanisms[2]. Reversing the same leg mechanisms enables the robot to takeoff after landing[2]. The dynamic perching and functional capabilities are demonstrated in Figures 5.i and Figure 5.ii. In Figure 5.i, SNAG is perched, recording data as an environmental sensor[2]. In the bottom left of the Figure (Figure 5.ii), SNAG approaches and lands dynamically on a perch using a bird-inspired near-horizontal approach path[2]. The hierarchical design of the bipedal perching

mechanism is shown in Figure 5.iii. Key biomimetic mechanisms include the digital flexor mechanism (DFM), which automatically closes the foot about the perch as the leg collapses and transfers the impact energy to supplemental squeeze force. Additionally, a locking ratchet that replicates the tendon locking mechanism (TLM) locks the leg and feet when perched[2], as in birds (section 1.1). Furthermore, as the feet (the end-effector) close around the perch, the 3D printed pointed claws engage with asperities on the branch surface, while the rough, rubber-backed, and wrinkled toe pads harness friction to absorb angular velocity and grip the surface[2]. In particular, absorbing the net angular momentum at contact was found to play an important role in perching success, which SNAG partially addresses through balancing at contact[2]. These features enable SNAG to perch on dirt, moss, and lichen-covered branches without observing surface properties and contact forces. To increase the robustness and adaptability of the robot, smart materials could further extend the capabilities of SNAG, e.g. by providing surface interaction force (haptic) feedback and surface property feedback to inform grasp force optimization[23] and better conform the end effector to complex surface features.

In general, the design of perching mechanisms for aerial robots is motivated by the desire to increase the landing capabilities beyond structured environments. As is expected, this work is motivated and preceded by earlier perching mechanisms[129]. While the general behavior and mechanism design is bioinspired, work in quadrotor perching has expanded to use an array of attachment methods beyond purely bioinspired solutions. These solutions generally include gecko tape, glue, suction cups, magnets, electro adhesion, micro spines, various gripper systems, reconfigurable frames, and penetration based features[130,131]. As sensing and compute capabilities have increase for mobile aerial robots, recent methods also include onboard sensing and planning in combination with new gripper designs for active and passive perching or grasping [131]. Grasping and perching robots are typically considered together because of the similarities between the two research areas. This close relationship has led the way towards designing robots that accomplish both actions with the same mechanism.

3.1 Smart materials for hierarchical mechanisms and perching robots

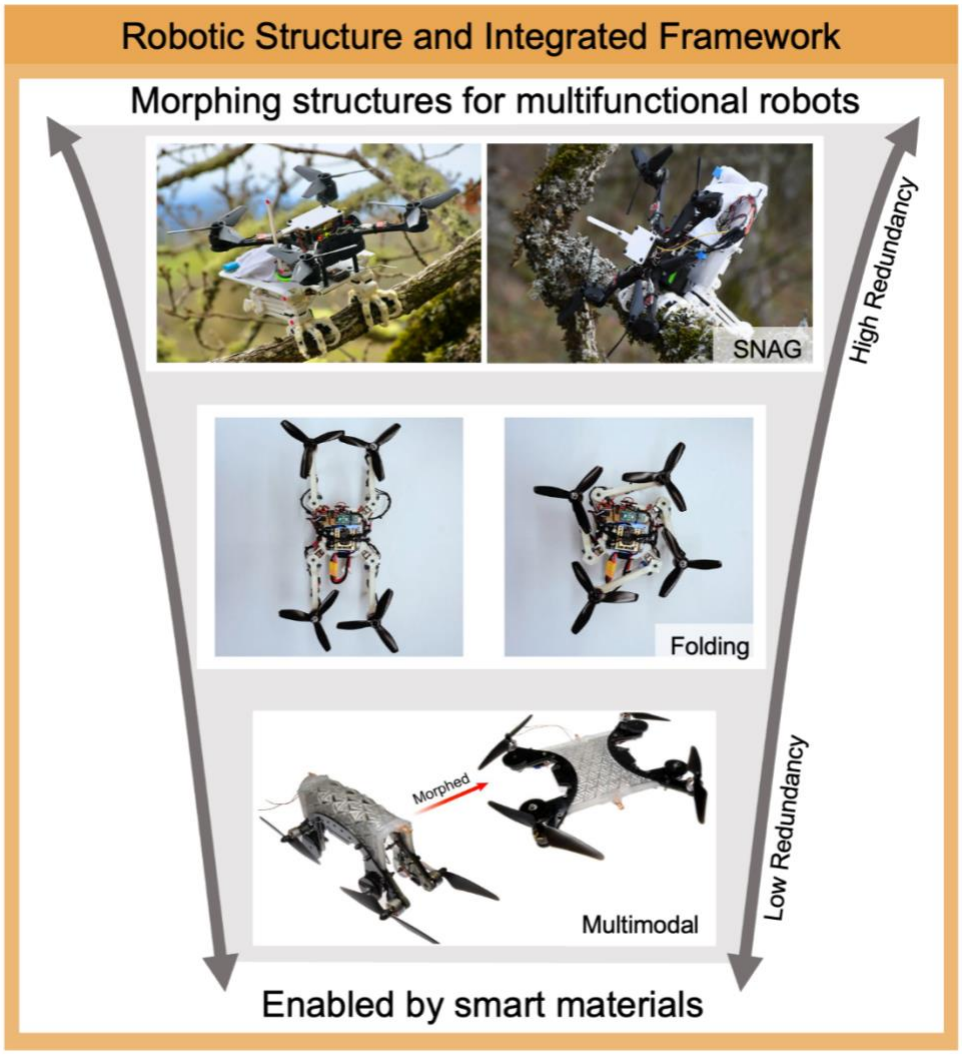

Figure 6:

Morphing structural materials will enable adaptability, new use cases, and better environmental resilience. *Variable stiffness morphing materials support multifunctional structures to enable multimodal robots and while reducing overengineering and redundancy* [2,132,133].

Developing robots that land on natural and manmade surfaces can extend mission length for tasks like surveillance or environmental monitoring[131]. In contrast to birds (section 1.1), robots typically require structured environments that are engineered for landing and takeoff (runways, grass fields, helicopter platforms, etc.). While SNAG demonstrates the state-of-the-art in robotic perching and grasping, smart materials could be used to improve perching performance. Two key opportunities are to minimize redundant structures by harnessing morphing smart materials with controllable stiffness (section 3.2) and to replace traditional actuators with artificial muscles embedded in the structure (section 3.3) to reduce weight complexity and improve overall robustness.

Aerial robots often employ duplicative, specialized structures to complete their locomotory function[131]. The occurrence of specialized and partly duplicative structures arises from a modular design approach in which each required function is addressed by a specialized solution combined with other dedicated solutions to create an entire system. While this approach is attractive from a design standpoint because function-separation reduces complexity arising from functional interaction, it leads to structural redundancies. For example, vehicles and robots may have both landing gear and a gripper which, if combined, could perform both all required functions with fewer parts.

Adaptive morphological changes based on smart materials can expand functionalities, improve dynamic performance, and reduce structural design redundancy[11]. These materials should have controllable variable stiffness and deform rapidly undergoing large and reversible strains with minimal energy loss, while being stiff enough to withstand the forces associated with flight, landing and takeoff[11]. A promising solution is controllable variable-stiffness structures[134,135]. Design approaches that fulfill these requirements include: 1) Combing soft materials with active materials that can change stiffness in response to temperature, electricity, pressure, or magnetic fields [11], 2) origami-inspired materials that can fold and lock to a desired configuration [11], and 3) bi-stable or multi-stable structures that can change shape and then maintain a desired shape with low energy consumption [11]. These materials enable new use cases of which we exemplify the potential with three robot designs with different levels of structural redundancy (Figure 6). As a first example, we consider SNAG (Figure 6, ”SNAG”), which contains a relatively high level of redundancy because the leg mechanism’s structure is neither integrated into the upper airframe of the aerial robot nor does it assist with aerodynamic or inertial control while flying (as birds do). While SNAG does reduce redundancy by employing its gripper as part of the landing gear, a more integrated robot design would make it more effective. The second example is the folding drone in the middle of Figure 6, “Folding”[133]. This morphing aerial robot folds its arms around its central body. The robot leverages an adaptive control strategy to expand flight capabilities, even during non-symmetric morphing[133]. Tight integration of the morphing structure with the novel control scheme reduced redundancy and expanded capabilities. Finally, we show a multimodal robot [132] at the bottom of Figure 6, “Multimodal”. This robot demonstrates a low level of redundancy by using a large, controllable, morphing structural airframe. As a result, nearly no redundant structure is needed to increase the function and capability of this aerial robot. This low level of redundancy is the result of its kirigami[136] (a variation of origami) inspired morphing composite body that can morph from a flat sheet to a load-bearing shape in a reversible fashion[132]. The top-down design and fabrication approach of origami robotic structures enables integrated system design[136]. More generally, integrated design solutions are key for developing new vehicle functions; for example, morphing wings that can fold into the body dynamically enable transitioning from air (flight) to water (swimming)[137]. These mechanical examples point to the potential of reducing redundancy across all functions.

A key aspect of multifunctional design is integration of the energy system into the structure. For example, batteries can be integrated directly into structural carbon fiber elements to create multifunctional energy storage composites (MESC) that are 15 times as rigid as traditional pouch cells[138,139]. Further developing these materials based on embodied energy design principles[140] can enable aerial vehicles to extend mission duration and overall mission functionality based on autonomy[131,141]. To achieve these improvements better integrated actuators are needed.

3.2 Applying artificial muscles for robot mechanism actuation

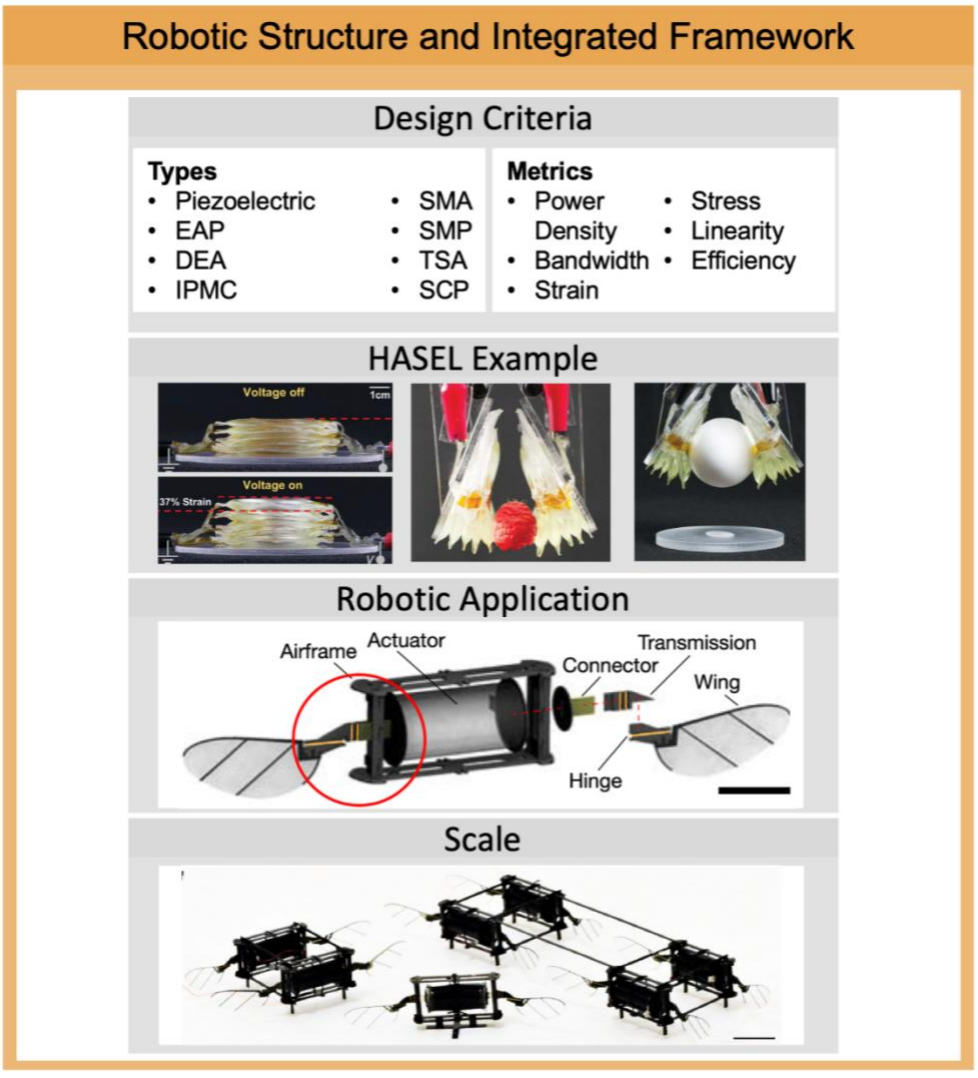

Figure 7:

Robotic artificial muscles are a promising technology to replace complex motor and servo driver mechanisms with more forgiving soft actuators [142]. *These artificial muscles are typically in one of eight categories and are evaluated using six different performance metrics* [142] *. A leading example is HASEL* [143]. *Artificial muscles have been applied to scalable small flapping robots* [144]. *Applying these technologies could improve SNAG's performance, decrease repetitive structures used in its design, and reduce assembly complexity.*

Current robots rely on complex mechanical design to achieve smart body functions. For example, SNAG uses a system of nylon tendons that transfer stored energy to trigger its grasping mechanism[2]. Indeed, many current robot grasping mechanisms rely on a complex sequence of tendons, pulleys, and actuators to drive mechanisms[145]. All these robots would benefit from scalable artificial muscle-based mechanisms that could be placed *in situ*, attached directly to the degrees of freedom that they operate to provide the dynamic force and length changes that are needed locally, as found in birds (section 1.1). Here, we will review current muscle types and design criteria in the context of applications.

Design criteria for artificial muscles in robots

The goal of robotic artificial muscles is to replace conventional electromagnetic actuators such as servo motors and the complex transmission systems required to deliver the dynamic (torque, force) and kinematic (displacement, rate, acceleration) output. Because artificial muscles are not a "one size fits all" replacement for traditional actuators, the intended application needs to be considered before implementation (Figure 7, "Design Criteria"). For example, a quick grasping mechanism as used in the legs of SNAG has different requirements than a gripper used for manipulating stationary objects. Each type of artificial muscle has distinct use cases according to its operating principle and characteristics[142]. Actuator types include piezoelectric actuators, dielectric elastomer actuators (DEA), ionic polymer-metal composites (IPMC), shape memory alloys (SMA), shape memory polymers (SMP), soft fluidic actuators, twist string actuators (TSA), and super-coiled polymers (SCP) (Table 1)[142]. The performance of artificial robotic muscles is traditionally evaluated using conventional actuator performance metrics[142]: power density, bandwidth, strain, stress, linearity, and efficiency[142]. The choice of the best artificial muscle technology requires trading off between these metrics, which we summarize in Table 1.

Table 1 Types of artificial muscles and the metrics used to evaluate them[142].

Type of Muscle	Function
Piezoelectric	Generate force when subject to an electric field through the converse piezoelectric effect.
EAP	Shape changing polymers which react to an electrical input. Two categories of EAP are DEAs and IPMC.
DEA (type of EAP)	Soft polymer coated on each side with different electrodes. Applying differential voltage results in compressive stresses.
IPMC (type of EAP)	Uses two layers of metal with a membrane in-between. The cathode metal attracts water and ions which results in bending in the membrane.
Shape Memory Alloy	Alloys which use the shape memory effect, which is the ability of a material to change shapes and then return to their original shape.
Shape Memory Polymer	Polymers which use the shape memory effect.
Soft Fluidic Actuators	These actuators convert energy, often in the form of a fluid or liquid, into mechanical motion.
TSA	TSAs convert rotation from a motor into a linear motion.
SCP	Uses twisted polymer threads to produce torque.

Metric	Definition
Power Density	Output work normalized by mass and actuation period
Bandwidth	Maximum trackable sinusoidal frequency
Strain	Change in length relative to initial length
Stress	Force generated normalized to cross sectional area
Linearity	Accuracy of a linear model to predict muscle output
Efficiency	Ratio of output power to input power

Application of robotic muscles into robotic structures

A long-standing challenge is to develop artificial muscle that can exceed skeletal muscle performance, promising candidates include dielectric elastomer actuators (DEA) and hydraulically amplified self-healing electrostatic (HASEL) actuators[146] (Figure 7, "HASEL Example"). HASEL actuators are a comparatively new technology that consists of a deformable shell filled with a liquid dielectric encapsulated in a structure with opposing electrodes. By applying voltage across the electrodes, the shape of the shell changes, resulting in a large actuation force[146]. In Figure 7, "HASEL Example", the actuator's linear performance, as well as its ability to manipulate delicate objects, is demonstrated[143]. The two different grasped objects show how a HASEL muscle gripper can seamlessly adapt to objects of diverse fragility and textures; this envelope is needed to make robotic structure approximate musculoskeletal system dexterity. In fact, the 37% strain of the HASEL actuator is already on par with skeletal muscle[143]. This emerging artificial muscle technology can thus improve multifunctional mechanism design[146].

The application of artificial muscles to flying platforms is in an early stage of development, with a few notable examples in microscale applications[147,148]. The potential of widespread use is exemplified by an insect-sized flapping microrobot (Figure 7, 'Robotic Application') that uses a soft artificial muscle to power its wings[144]. The 155 mg flapping-wing robot uses a dielectric elastomer actuators (DEA) to power its flight. Each DEA weighs less than 100 mg with a power density of 600 W/Kg. The multifunctionality of this actuator is exemplified by how actuator softness increases the robustness of the flapping wings to collisions. At larger scales, electromagnetic servo actuators remain predominant. However, as demonstrated in this flapping robot, it is possible to scale small artificial muscles by recruiting them in parallel to meet the demands of larger platforms (Figure 7, 'Scale')[144]. A major open challenge is linearizing muscle actuator performance so they are more amendable to robust closed-loop control. Provably stable control systems require linearity, which electric motors excel in across scales[144]. Another major open challenge remains scaling the favorable properties of artificial muscles up to aerospace scales[142]. Looking ahead, use cases for future artificial muscles would be even more compelling if they can also replicate other unique properties of natural muscles. These include synergy, in which groups of muscles contribute to particular movements[149]; recruitment, the ability to vary how many muscle fibers in a muscle are activated[150]; their ability to self-heal; and practically silent operation. To achieve these, artificial muscle development needs to push the boundaries of material science (e.g. compressible materials with high dielectric constant and low hysteresis) and fabrication methods [151]. As a result, extensive material development is still required to realize the full potential of artificial muscle integration[142,146,148], especially at larger aerospace vehicle scales. One case study we can look at are artificial muscles in flapping robots, which we briefly discuss below.

Comparing artificial robotic muscles with traditional actuators in flapping robots

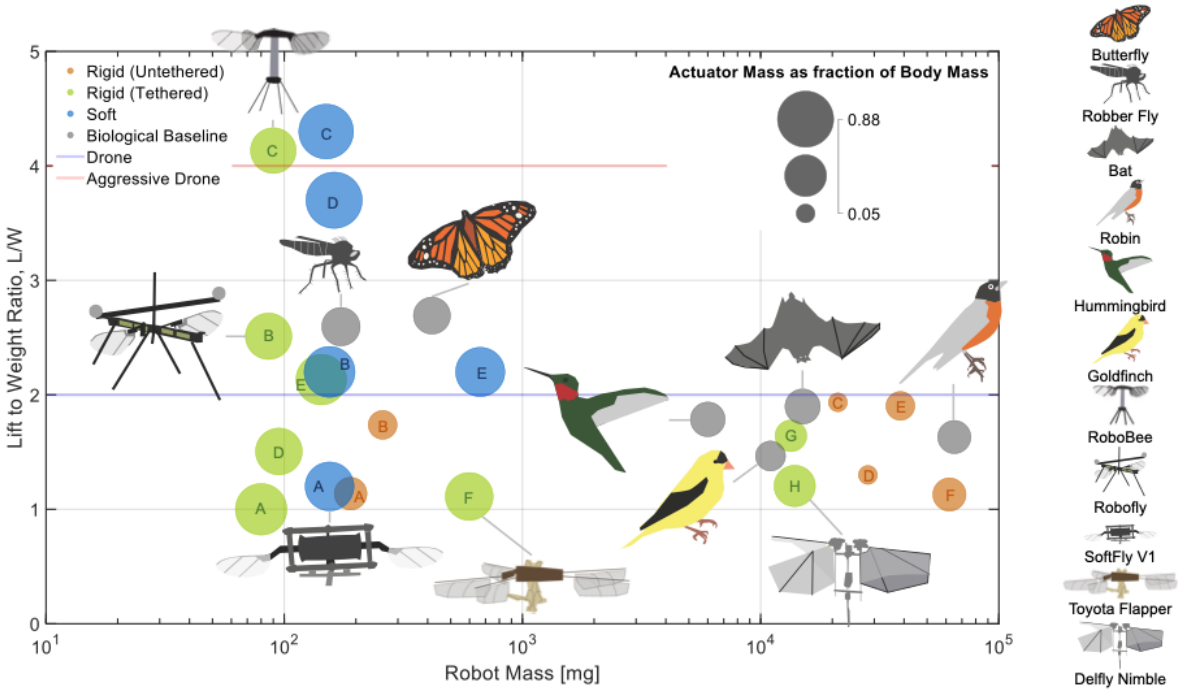

Figure 8 *A case study in applying soft acutators to aerial robots. A comparison of existing flapping robots with both artificial muscles and rigid actuators. Biological baselines are included to give context for the robotic prototypes. All muscle actuator robots are tethered during flight. Data and sources available in Table 2.*

Small-scale flapping robots provide a unique opportunity to compare the use of robotic muscle actuators to show their benefits and shortcomings. This stems from sub-gram flappers being one of the areas in aerial robotics to have used these new actuators and the lack of flying robots that use artificial muscles as a primary means of propulsion. To demonstrate the relative performance of different types of actuators in flapping robots, Figure 8 compares robots using traditional actuators (motors, piezoelectric, electromagnetic, etc.) with a few examples of robots with artificial robotic (soft) muscles, as well as several biological baselines. In comparing to existing robots, we can see that the most capable muscle actuators achieve higher lift-to-weight ratios compared to existing flapping robots. This achievement suggests the potential for highly advanced robotic fliers that benefit from the advantages that robotic muscles actuators bring. By combining higher lift-to-weight ratios with the benefits of soft robotic muscles, flapper robots with artificial muscles can perform somersault, other acrobatic maneuvers, and recover from collisions that rigid robots cannot[147]. High lift-to-weight ratios are desirable because they are associated with higher maneuverability. Combining high maneuverability with robust mechanical design is an ideal combination to make future robots highly capable in varying flight conditions and environments because of the resulting durability. Unfortunately, these flapper robots are still tethered. As a result, future challenges for using artificial muscles for powered flight include designing the energy storage, power electronics, and flight control systems that enable controlled untethered flight. While flappers with soft actuators have a higher payload than their rigid counterparts[147], their maneuverability will be significantly affected unless engineers can maintain similar lift to weight

ratios. Finally, based on the examples shown in Figure 8, as flapping robots and their biological counterparts scale, their lift to weight ratios decrease. As a result, the larger robots and animals are less maneuverable because their maximum acceleration is lower. All in all, soft robotic actuators have the potential to bring improvements to small flapping robots, but significant engineering development is needed to realize their improvements over traditional actuators.

Table 2 Data for Figure 8. Table data adapted from various sources including research and review papers[147,152–163].

	Weight [mg]	Max Lift [mg]	Lift to Weight Ratio	Actuator Mass [mg]	Actuator Mass/ Robot Mass %	Figure Reference
Traditional Actuators						
Tethered						
EM	80	80	1	58	73%	A
Robofly	86	216	2.5	50	58%	B
RoboBee	90	372	4.1	50	56%	C
Bee+	95	143	1.5	56	59%	D
Robofly (four wings)	143	305	2.1	100	70%	E
Toyota Flapper	598	665	1.1	368	62%	F
fwMAVS	13400	22000	1.6	3180	24%	G
Beetle Type	13900	16735	1.2	6280	45%	H
Untethered						
RoboFly Wireless	190	216	1.1	50	26%	A
BigBee	259	450	1.7	50	19%	B
DelFly 2	21100	40816	1.9	1000	5%	C
DelFly Nimble	28200	36660	1.3	1430	5%	D
Butterfly	38600	73469	1.9	7500	19%	E
Robotic Hummingbird	62000	70000	1.1	16800	27%	F
Muscles Actuators						
SoftFly V1	155	186	1.2	100	65%	A
SoftFly V2	155	341	2.2	110	71%	B
SoftFly V3-6	150	645	4.3	125	83%	C

SoftFly V3-20	162	601	3.7	143	88%	D
SoftFly V2 Four Part	665	302	2.2	440	66%	E
Baseline						
Drone			2			
Aggressive Drone			4 to 7			
Hummingbird			>1.5			
Flies			2-3.5			
Biological Baselines						
Robber Fly	173	449	2.6	65	38%	
Butterfly (Danaidae)	417	1122	2.7	146	35%	
Hummingbird	6000	10714	1.8	1800	30%	
Goldfinch	11000	16122	1.5	2300	21%	
Bat	15000	28469	1.9	4700	31%	
Robin	65000	106020	1.6	17600	27%	

4 Grasping Bioinspired robotics vignette 3: AGR's aerial grasping robot mechanism for fast and compliant airborne interaction

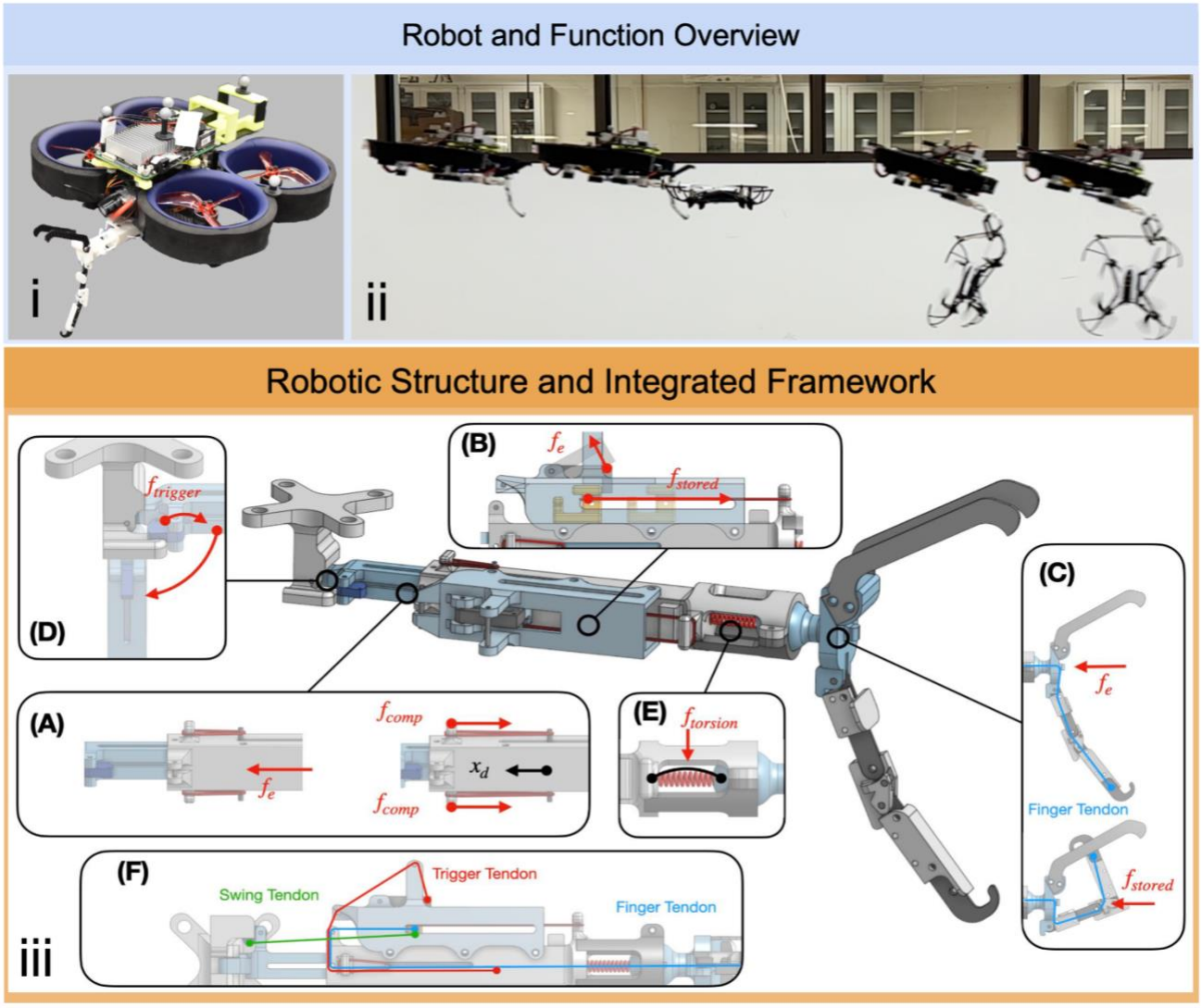

Figure 9:

The aerial grasping robot (AGR) catches target drones in flight using a passive grasping mechanism that closes in milliseconds. ***(I)*** *Grasping robot is a 550 g quadrotor that can catch an 85 g target drone. Onboard the drone is a PX4 autopilot board and Intel UPboard companion computer, which receives a trajectory from a base computer.* ***(ii)*** *A composite image showing a successful grasp with a safe recovery.* ***(iii)*** *Detailed overview of the gripper mechanism showing tendons and passive elements. Applying a small force at the end of the gripper activates it by releasing stored energy.* [3] *While the lettered callouts are kept here to demonstrate gripper details, full function and videos can be found in the paper.*

Robotic manipulators should be thoroughly instrumented to autonomously complete their tasks[164]. To accomplish this, we still need significant work in robotic manipulation[164] and soft robotics[128] to drive future areas of research to enable an instrumented aerial grasping mechanism. The Aerial

Grasping Robot (AGR) (Figure 9.i) uses a passive grasping mechanism to catch objects and drones in flight (Figure 9.ii)[165]. The design of AGR builds off similar bioinspired principles as SNAG (Section 3) by using passive mechanisms to control and release the trigger to close the gripper. The mechanism utilizes stored energy in pre-stretched rubber bands (Figure 9.iii.B) to power the underactuated finger (Figure 9.iii.C) for a grasping sequence. Upon impact, the main linear sliding element (Figure 9.iii.A,F) of the mechanism acts as a suspension, and the movement of this suspension is tied to a trigger, releasing stored potential energy and closing the under-actuated finger. In-flight grasping is difficult because the collision impact of the grasper cannot exceed the control authority of the main drone to avoid any irrecoverable disturbance. Further, the pursuit drone needs to close its grasper around the target drone sufficiently quickly to avoid ejection due to the target drone bouncing off the gripper. To work within the grasping ejection constraints, the AGR gripper fully closes in ~10 ms and then applies maximum grasping force. The current gripper uses a fixed gripper attached to the bottom of the drone to pursue a moving target.

Currently, grasping robots generally allocate a large mass percentage to their grippers, unlike birds which are more efficient in their mass allocation. In the next section, we briefly discuss this comparison and how it should motivate engineers and designers to develop and apply smart materials.

4.1 Mass Allocation Comparison between Robots and Birds

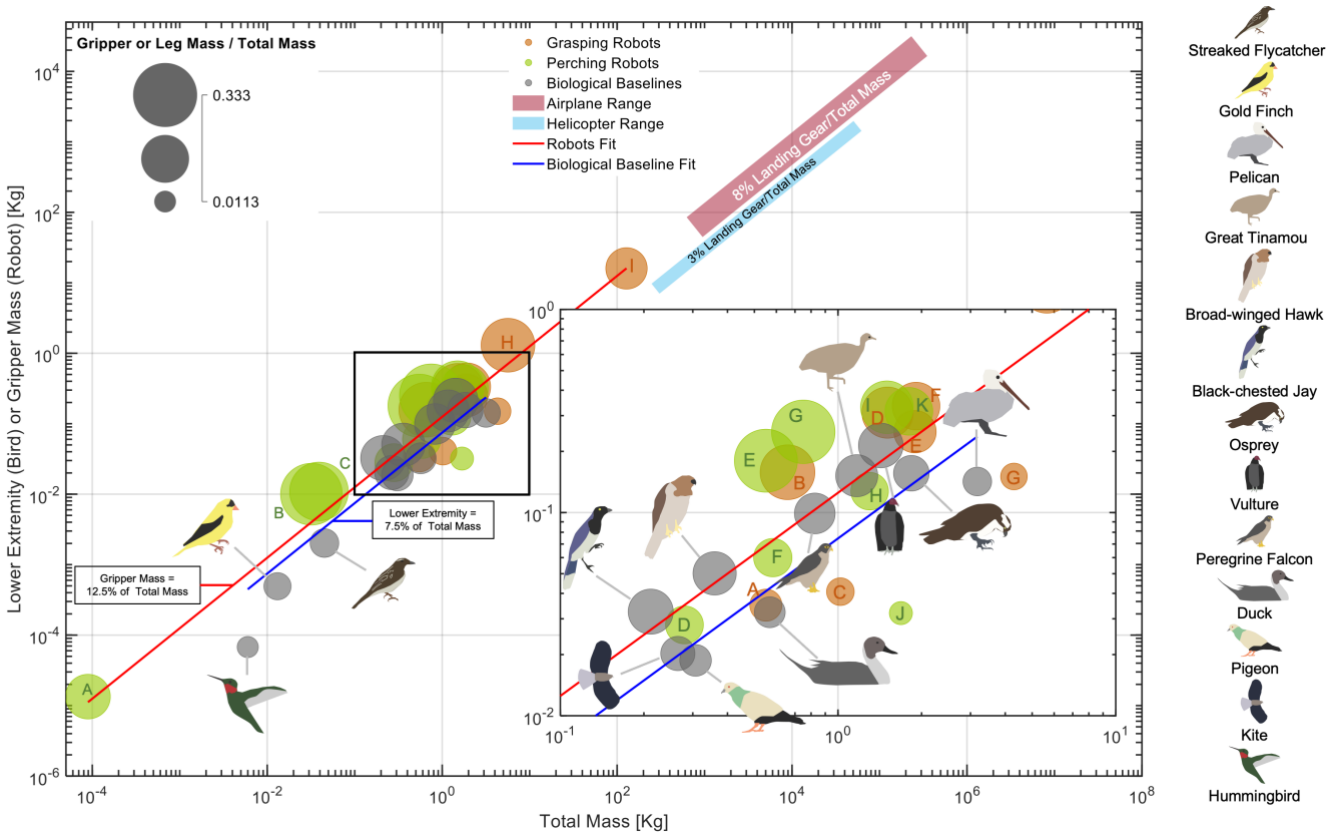

Figure 10 *Grasping and perching robots consistently allocate more of their mass towards their manipulators relative to the lower extremities of their avian biological counterparts. This figure shows a comparison of leg or gripper mass as a proportion of total mass of robots and birds across varying mass scales. Biological baselines are included to provide context for the robot prototypes. Letters in circles correspond to robot details in table 3. All data and sources available in table 3.*

A notable feature of the aforementioned Aerial Grasping Robot is the low mass percentage allocated to the gripper, only 6%. This is half of the typical mass allocation of grippers in grasping and perching robots and on par with the mass percentage allocated towards the lower extremities of birds. However, overall, grasping and perching robots typically allocate a larger fraction of their mass towards their grippers compared to birds across various mass scales. We illustrate this in Figure 10, where we compile the total masses, lower extremity (bird) or gripper mass (robot), and mass ratios for birds, robots, and a few other aerial vehicles such as airplanes and helicopters. Across various bird species, the lower extremities of the birds make up 7.5% of the total mass of the bird whereas in robots 12.5% of the mass is used for the gripper. Important to note is that this comparison is only for the grippers of robots, whereas the lower extremities of the birds are highly multifunctional, as we have discussed throughout this work. This conclusion demonstrates the motivation for developing new smart materials that can enable robot designers to allocate less weight to the grippers and more weight to other critical drone components, such as batteries, actuators, or computer. More efficient smart materials that combine functions could also lower the overall mass entirely, leading to performance benefits such as better maneuverability and efficiency. Specifically, incorporating sensing and actuation, as discussed in

the forthcoming section, into smart materials for aerial robots could be a means to close the gap between man-made robots and birds.

Table 3 *Data on robot and bird mass allocations corresponding to Figure 10. Data compiled from various sources*[131,165–167]*. Robot names adapted from Grasping and Perching review by Meng et al* [131]*. Figure reference for data points in Figure 10.*

	Name	Total Mass [Kg]	Leg or Gripper Mass [Kg]	Leg or Gripper to Total Mass Ratio	Figure Reference
Grasping					
	Aerial Grasping Robot	0.550	0.04	0.06	A
	Avian-inspired Aerial Manipulator	0.658	0.16	0.24	B
	Wasp-pedal-carrying Aerial Manipulator	1.020	0.04	0.04	C
	Origami-inspired Aerial Manipulator	1.507	0.31	0.21	D
	Folding-arm Aerial Manipulator	1.894	0.25	0.13	E
	Aerial Torsional Manipulator	1.910	0.33	0.18	F
	Helicopter-linkage-hand System	4.300	0.15	0.04	G
	Dual-arm Aerial Manipulator	5.652	1.30	0.23	H
	Industrial Aerial Manipulator	128.000	16.00	0.13	I
Perching					
	Flap-wing Electro adhesive Perching Mechanism	0.000089	0.000013	0.15	A
	Magnetic Extended-leg Perching Mechanism	0.032	0.01	0.31	B
	Thrust-assisted Perching Mechanism	0.039	0.01	0.28	C
	insect-inspired Perching Mechanism	0.280	0.03	0.10	D
	Three-directional Perching Mechanism	0.550	0.18	0.33	E
	Gecko-inspired Perching Mechanism	0.583	0.06	0.10	F
	Parrotlet Perching Mechanism	0.750	0.25	0.33	G
	Untethered Electroadhesive Perching Mechanism	1.300	0.13	0.10	H
	Reconfigurable Perching Mechanism	1.500	0.33	0.22	I
	Adaptive Microspine Perching Mechanism	1.684	0.03	0.02	J
	Vacuum-cup Perching Mechanism	1.800	0.32	0.18	K
Biological Baselines					
	Green Hermit Hummingbird	0.006	0.00	0.01	
	Goldfinch	0.013	0.00	0.04	
	Streaked Flycatcher	0.045	0.00	0.04	
	Black Chested Jay	0.212	0.03	0.15	
	Hook-billed Kite	0.265	0.02	0.08	
	Pigeon	0.307	0.02	0.06	
	Broad winged Hawk	0.360	0.05	0.14	
	Duck	0.568	0.03	0.06	

Peregrine Falcon	0.825	0.10	0.12
Great Tinamou	1.168	0.15	0.13
Vulture	1.426	0.21	0.15
Osprey	1.837	0.16	0.09
Pelican	3.174	0.14	0.04

4.2 Smart materials for aerial grasping robots

Aerial grasping drones have practical applications, such as removing malicious drones from sensitive airspaces. In contrast to other destructive methods including brute force or projectiles, this grasping method disables the target drone without excessive debris. However, more instrumentation and better gripper materials are needed to improve the capabilities of the AGR mechanism and increase its autonomy. Smart materials provide the opportunity to embed sensing into a gripper mechanism and to create fast actuating, compliant structures that increase the likelihood of a successful capture. In this section, we discuss the most relevant types of sensing for aerial grasping mechanisms (Figure 11) and then discuss how to leverage soft robotic principles (Figure 12) to improve the performance of robotic grasping mechanisms like that on AGR.

4.3 Sensorized gripper for autonomous grasping

The adaptability and robustness of autonomous aerial grasping systems can be generalized by integrating advances in manipulation and soft robotics. In comparison to most robotic hands and grippers, aerial grasping places an emphasis on minimizing weight and fast response. In the context of AGR, the two most relevant areas for embedded sensing in the grasper are 1) proprioception and 2) tactile sensing (Figure 11.A, “Sensorized Grasper”). For embedded proprioception, curvature and length sensing are most relevant to capture the changing shape of the grasping mechanism under loading. Tactile sensing is important for knowing how the gripper is interacting with its target. To show how this sensing could be accomplished, we consider current sensing modalities used for manipulation in soft robotics (Figure 11, “Types of Sensors”, “Types of Sensing”)[168].

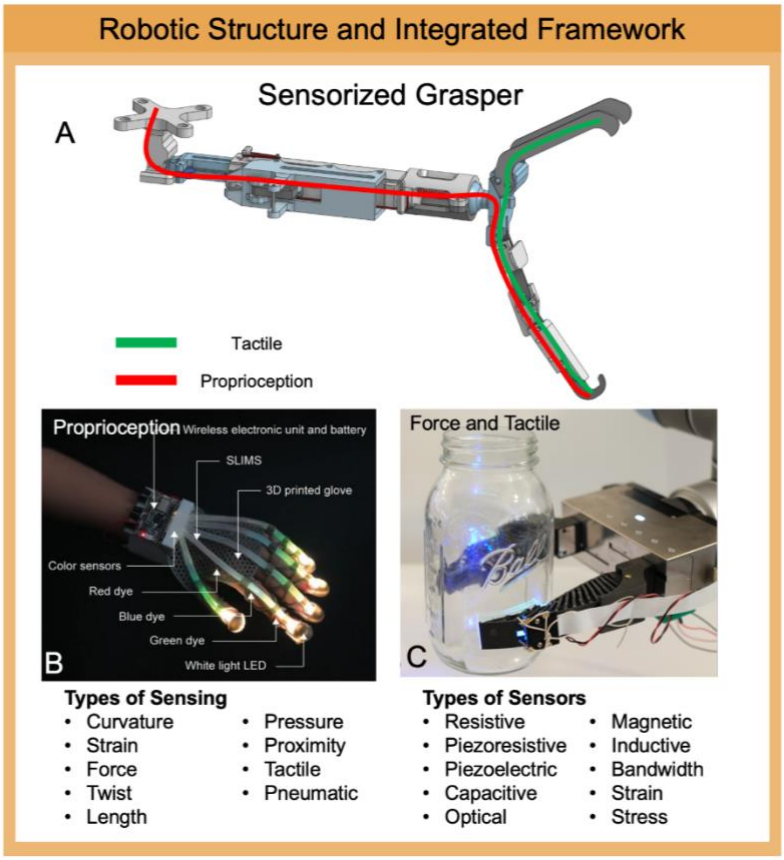

Figure 11: To perceive their environments and the target, grippers must be sensorized. Smart materials can be used for local proprioception, force, and tactile sensing. *[A] The ideal regions for the two desired types of sensing are depicted by the colored lines and include proprioception and tactile sensing. [B] A soft skin for human hands demonstrates optical based proprioception* [169]*. [C] A compliant gripper (GelSight Fin Ray) with GelSight finger tips can infer forces and detect touch using optical sensing* [170]*. [Bottom Row] Types of sensing and sensors typically used in soft robotic grippers* [168,171]*.*

Proprioception improves grasper trajectory control

A major design improvement of aerial graspers is to actively control joints so that the motion of the gripper is decoupled from the aerial robot flight trajectory. This decoupling would enable the robot to fly desired trajectories while the position and orientation of the grasping end-effector is optimized as well. This requires feedback control in the grasping mechanism, so it can compensate for linear and angular motion of the aerial robot and thus optimize the desired orientation of the end effector. This is not unlike how camera gimbals use inertial measurement units (IMU) for stabilizing and orientating the camera[172]. Other examples include robotic arms, which use joint sensors (e.g. potentiometers) to calculate inverse kinematics[173]. Critically, combination of orientation sensors with torque sensors[174] would enable the estimation of the mass properties of the captured object (beyond inertial model based approaches). These approaches can be improved for aerial robotic grasping mechanisms by compensating for the significant deformations that

compliant soft robotics and bioinspired mechanisms typically undergo (section 1.1), especially while dynamically colliding with a target to grasp it.

Implementing fiber optic sensing through the linkages of a gripper mechanism is another suitable sensing solution that could be directly integrated into the materials of the mechanism. Traditional fiber optic sensor systems are inextensible and designed for rigid structures with minimal strain, so these sensors would struggle with the complex geometry of the aerial grasping mechanism[175]. Another challenge of implementing fiber optics sensors in mobile robotics is the size and weight of the interrogator, which is needed to analyze the optical signal from fiber optic cables[176]. These challenges are resolve by new designs based on stretchable fiber optic sensors with flexible elastomeric lightguides, combined with LEDs and optimized dyes. By exploiting optical effects, it is possible to measure structural deformations in a more flexible and portable fashion (Figure 11.B, "Proprioception")[169]. Currently, these sensors are limited to a range of tens of centimeters and are larger in diameter than traditional fiber-optic sensors. While a benefit of this new approach is the flexibility of the optical fibers, additional benefits will be realized when the sensors are miniaturized to their theoretical limits. Smaller form-factors will increase their versatility and usefulness, especially when combined with composite fibers that form load paths in robotic structures.

Tactile sensing improves grasping after impact

While proprioception is critical before the collision of the grasper, after impact, tactile sensing becomes equally important for dexterous manipulation. Tactile sensing enables detection of successful contact initiation and grasp effectiveness. After a successful grasp, the robotic system and the grasped object become one, and estimating the new mass properties of the combined system is crucial to optimally control its flight path. Two general approaches that would enable the system to acquire this information. One is to estimate mass property using the telemetry and a model of the thrust of the main drone, which requires assumptions about inertial properties[177]. The other is to incorporate tactile sensing capabilities into the gripper structure.

Tactile sensing innovations are among the popular areas in robotics research because they are thought to be critical for achieving human-level robotic manipulation[164,168]. While it is beyond scope to provide a comprehensive review, we focus here on one of the most promising recent technologies[178]. GelSight is an optical tactile sensor that uses a camera to measure the deformation of a soft elastomeric surface[178]. From the image, the sensor can infer contact stresses and slip[178]. Figure 11.C, "Tactile", shows a robotic gripper with a GelSight sensor at the tips of a fin ray gripper[170]. A benefit of this sensing approach is that the compliant nature of the elastomer enables sensing as it deforms around a grasped object. Such compliance is necessary for robust high-speed grasping. Challenges, especially for dynamic aerial grasping applications, include sensor packaging and the need to process tactile data rapidly on the wing. Integration challenges continue to impede the adoption of tactile sensing in robotics, especially in small aerial robots. Smart

materials with embedded sensing offer the opportunity to mitigate wiring and communications challenges. They can reduce the required numbers of cables and interconnects, allowing sensors to be applied to more complex geometries and to deformable structures, which have been notoriously difficult to instrument with traditional sensors[168]. This also has the potential to reduce the total mass of the system. To illustrate the potential, we consider compliant structures for fast catching in the next section.

4.4 Compliant structures for fast catching

Aerial grasping is a challenging endeavor because the action is nearly instantaneous with little margin for error. While flight testing the AGR, two key design requirements emerged: fast grasping and contact force minimization[3]. Although the gripper on AGR actuates quickly, it is stiff, leading to relatively high impact forces that can result in unsuccessful grasping attempts due to ejection (object bouncing in the grasper)[3]. Ideally, the gripper should be sufficiently compliant to conform to a target, gradually reducing the relative velocity to reduce peak contact force as in a suspension system. Soft robotics grasper technology based on bistable compliant structures as well as phase-change based particle/layer jamming can improve dynamic grasping.

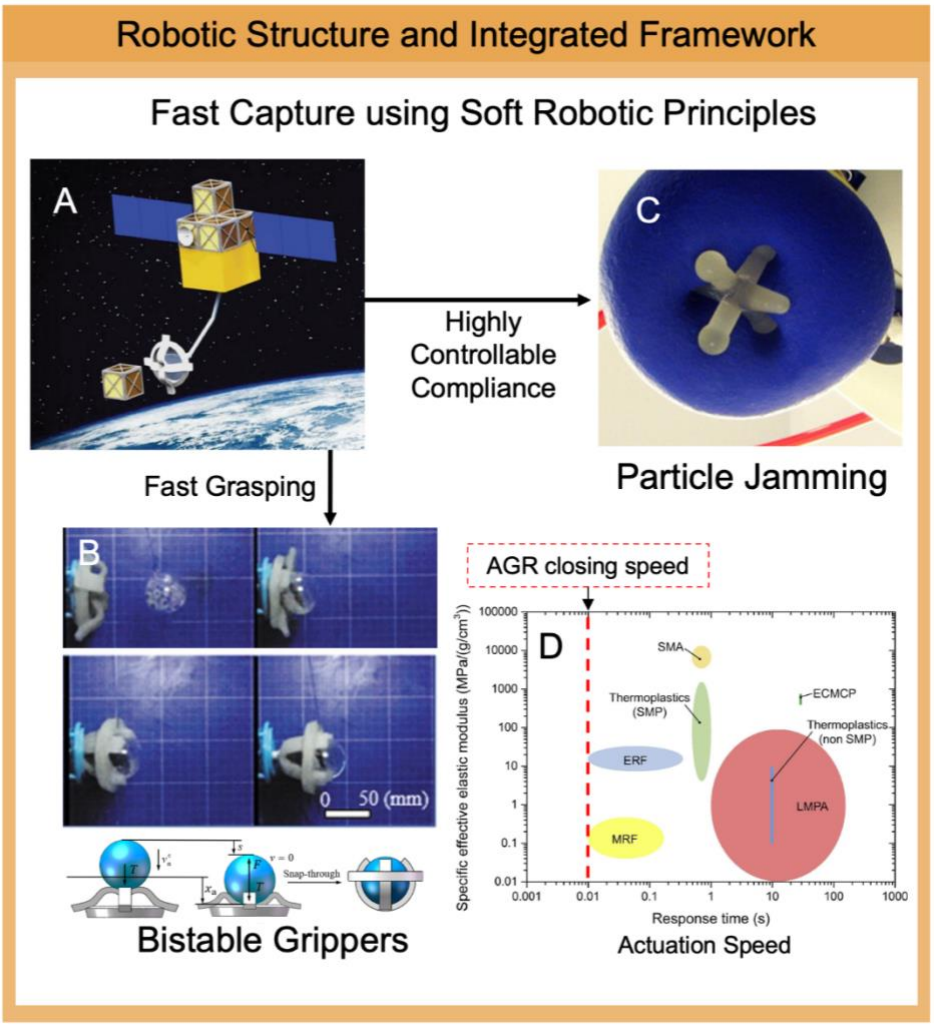

Figure 12 For optimal aerial grasping, the gripper must be fast closing and able to dampen impacts. Smart materials can be integrated to incorporate fast and compliant grasping mechanisms. *Two soft robotic principles should drive material development for aerial grasping robots. Future materials should be fast and highly controllable, compliant materials. [A] A proposed fast capture mission in space* [179]*. [B] A bistable gripper that can close quickly and conform to a variety of object shapes. The top set of images are a time sequence of the gripper actuating and the bottom set are a similar CAD sequence of the gripper activating.*[179] *[C] A particle jamming gripper with high variable compliance, extreme conformability, and high grasping forces* [180]*. [D] A plot of the response times of existing materials used in soft robotic grippers* [135]*.*

Current soft grippers designed for manipulation[164] are relatively slow and heavy for applications in aerial dynamic grasping systems[135], illustrated in Figure 12 "Actuation Speed". The red line represents the closing speed of AGR's gripper; current materials used for soft grippers are much slower[135]. The technologies that currently come closest are electrorheological (ER) and magnetorheological (MR) fluid-based grippers[171]. We therefore consider two soft robotic principles below to enable fast grasps. The first is bistable structures and the second is particle

jamming for conforming during grasping. An ideal new smart material would combine the principles of these two concepts into one usable material or structure capable of fast capture.

Bistable materials and structures offer a solution for fast grasping. They can be loaded to a stable, high potential energy state and then upon triggering, snap to a second stable state with the release of energy (similar to how the venus flytrap traps insects). A robotic example of this grasping principle is shown in Figure 12, “Bistable Grippers”[179]. This gripper is designed for a conceptual high-speed space grasping task (Figure 12.A). When the target hits the mechanism, a force is applied to the gripper, which quickly closes around the grasped object[179]. The trigger force is tunable, by adjusting the initial deformation of the gripper, it is possible to adjust the grasping energy threshold[179]. An overall benefit of bistable materials is that they often do not need any external actuation or sensor input during grasping. Using the bistable principle in a composite material for the fingers of an aerial grasping mechanism could contribute to a rapid, secure grasp about the target object. To absorb collision energy further, particle jamming principles could provide a soft palm that quickly conforms around the target and firms.

Particle jamming systems are notable for their ability to (1) dynamically change from a highly deformable state to a nearly solid state and therefore (2) grasp objects with complex geometries [180]. These two principles make jamming grippers nearly universal grippers. As the membrane bag enclosing the granular material collapses, e.g. under the actuation of a vacuum, the packing volume lowers slightly and the gripper transitions to a near solid state. The tight conformation allows the gripper to lift and handle a wide range of object sizes and loads than possible without jamming[180]. An example that demonstrates the ability to conform to complex geometries is shown in Figure 12 “Particle Jamming”[180]. Integrated jamming grippers with an impact-absorbing gripper "palm" in flying systems that rapidly pull a vacuum (within 10 ms or so) could improve grasp stability and collision energy dissipation.

The principles for designing better aerial grasping mechanisms by improving the underlying structures to be fast grasping and compliant has applications in designing new bioinspired landing gear[181] for aerospace vehicles. Such new landing gear designs will need to quickly absorb significant energy during short or vertical take-off and landing. Overall, we argue that improving robotic grasping mechanisms and structures has broader implications in aerospace applications than perhaps originally thought, especially in energy absorbing structures.

5 FalconBot and aircraft conceptual design framework for multifunctional smart material development

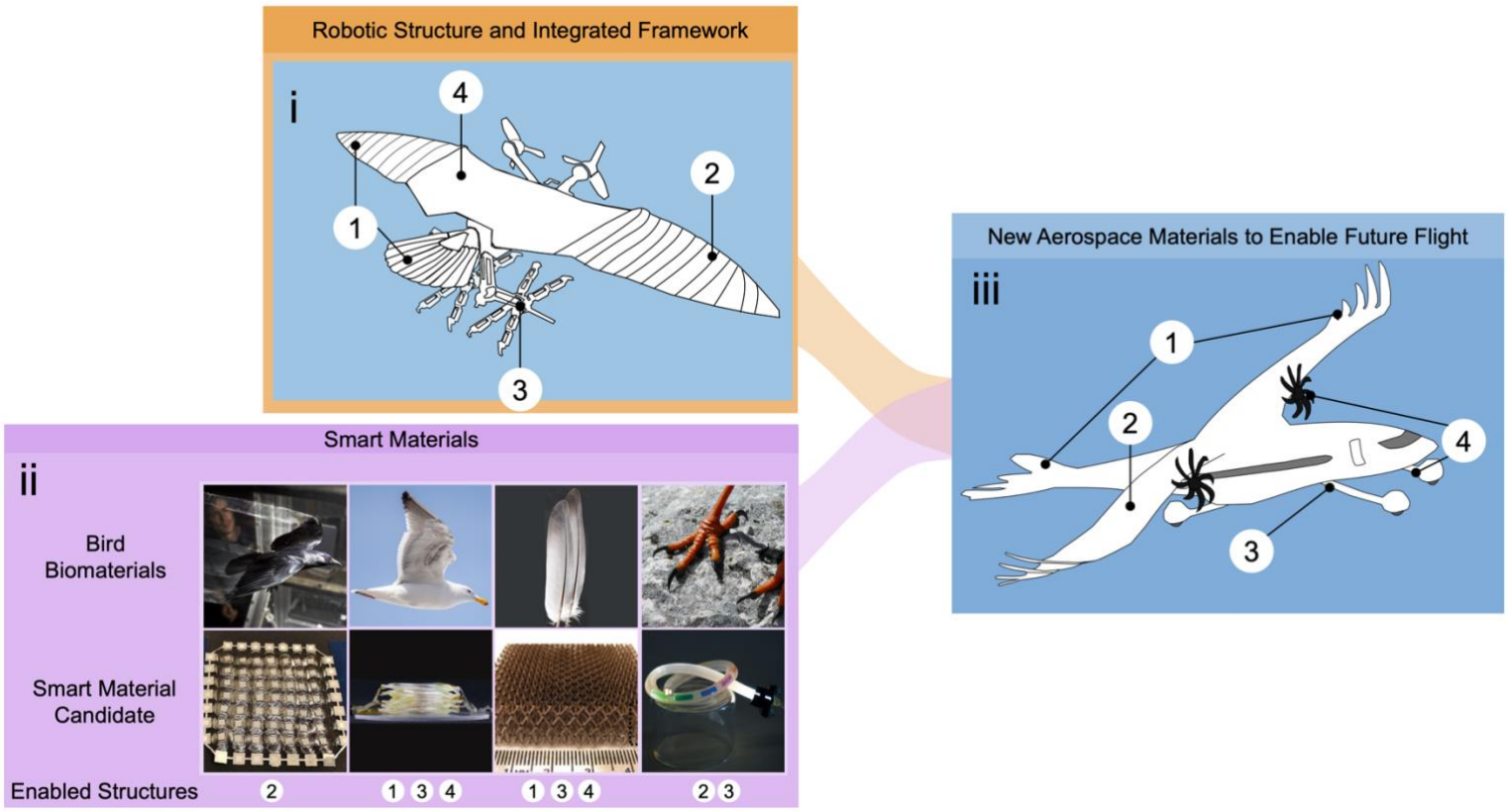

Figure 13:

FalconBot (i), and its aircraft equivalent (iii), is a conceptual framework that synthesizes biohybrid (PigeonBot), biomimetic (SNAG) and bioinspired (AGR) avian design principles as inspiration for developing new multifunctional smart materials*: (1) Smart wing structures with wing morphing for supermaneuverable flight, (2) Embedded sensing for control and autonomy, (3) dynamic pursuit for aerial grasping, and (4) vertical takeoff and landing (VTOL) with a multifunctional gripper.* ***(ii)*** *Illustrations of smart materials that can mimic some of the avian solutions:* ***First Column*** *top, sensing flow with wing and feather structures, illustrated by a visualization of the wing and tail tip vortices in bird flight [Photo Credit Aron Hejdström]. Bottom, A flexible pressure sensing skin* [127]*.* ***Second Column*** *top, dynamic actuation of a soft morphing wing by the avian musculoskeletal system [Photo Credit George Roderick]. Bottom, the HASEL artificial muscle capable of generating similar force levels and length changes* [143]*.* ***Third Column*** *top, feather hierarchical structure enables load sharing, interlocking, and passive aerodynamic filtering [Photo Credit Laura Matloff/Kenneth Hoffmann]. Bottom, ultralight microlattice materials enabled by their hierarchical structure* [70]*.* ***Fourth Column*** *top, Peregrine falcon foot [Photo Credit Piers Cavendish]* [182]*. Bottom, flexible fiber optics can provide proprioception* [169]*.* ***iii*** *Equivalent aerospace concept vehicle, integrates designs inspired by the Airbus Bird of Prey concept* [183] *and the Phratcyl MACROBAT*[184]*, with the proposed multifunctional smart materials. The callouts represent the most similar function to the robot counterparts reviewed. The bioinspired landing system enables more robust (short or) vertical takeoff and landing on rudimentary runways and helicopter platforms.All images reproduced with permission.*

5.1 FalconBot framework for multifunctional smart material development

The FalconBot conceptual aerial robot design integrates the biohybrid (PigeonBot), biomimetic (SNAG), and bioinspired (AGR) avian design principles that we reviewed for each robotics vignette (Figure 13.i). It consists of: (1) a multifunctional morphing wing and tail structure for super maneuverable flight, (2) embedded wing sensing for fly-by-feel control to robustly increase the flight envelope, (3) a grasping mechanism used for dynamic aerial grasping and perching, and (4) multi-rotor vertical takeoff and landing capabilities (since wing-flapping has not yet been shown to scale across aerospace scales). Examples of specific multifunctional smart material solutions for biohybrid, biomimetic and bioinspired avian design principles in our review are given in Figure 13.ii. Embedded aerodynamic pressure, shear, and flow sensing as well as structural strain, stress and vehicle-scale deformation sensing in the skin and the fusion of this information in the closed-loop control loop enables the morphing wing and tail to adapt robustly to the task at hand under challenging external disturbances. To actuate the multifunctional morphing surfaces, robotic legs and end effectors as well as the vertical takeoff and landing mechanisms, artificial muscles like HASEL or DEA[146] could be used in place of traditional electric motor based actuators. Furthermore, hierarchical cellular composite materials with microscale fasteners based on microlattice structures[70] could furnish the necessary lightweight, multifunctional structures needed for morphing. Finally, smart materials could decentralize communication needs in the structure, enabling local interpretation of sensor data, reducing sensor packaging challenges, increasing communication bandwidth, and decentralizing computation requirements[185]. Whereas testing these capabilities is feasible on aerial robotics platforms, which makes them uniquely capable testbeds for multifunctional smart material development, ultimately these technologies will also improve future aircraft across aerospace scales (Figure 13.iii).

Further development of smart materials described throughout this work can address the technical challenges to realizing the FalconBot concept. For flight, these challenges include morphing wing surfaces with better morphing capabilities that are manufactured from easily procured materials. Existing solutions use materials that would not stand up to harsh requirements of robots in the real world[161], so commercial versions of research prototypes have begun to investigate non-biological alternatives[186]. For perching and grasping, traditional tendon driven mechanisms could be replaced by more easily manufactured grasping and perching mechanisms that leverage distributed actuation and the forgiveness of soft actuators. Finally, expanding sensing beyond traditional drone sensors could enable more dependable sensing when future aerial robots interact with their environments. To address this, material designers should focus on more easily accessible and modular materials to seamlessly integrate into existing and future robotic mechanism design. These challenges are beginning to be addressed by the literature presented throughout this work. All in all, these technical innovations together would enable FalconBot to be a dependable aerial robot platform beyond a one-off prototype.

We propose that multifunctional robotic concept designs such as FalconBot provide an ideal framework for incorporating and testing new advances in structures, materials, sensors, and actuators. This is exemplified by the rapid research and development cycle of the reviewed biohybrid, biomimetic and bioinspired aerial robot vignettes, which successfully translated and flight-tested recently discovered avian design principles to demonstrate their engineering use. A key benefit of small autonomous aerial robots is that their design and fabrication cycles are much more rapid and can involve greater risk-taking at lower cost. The overall cost of fabrication and of conducting tests is low, even in the event of frequent catastrophic crashes, which speeds up research and development. Conveniently, small natural fliers, also impose a premium on integration and multifunctional capabilities to reduce volume and weight. Admittedly, scaling to large vehicles will impose additional challenges not encountered with small robotic fliers, in particular: affordable large-scale airworthy manufacturing of multifunctional components. Given these burdens, it is especially valuable to first flight-test innovations at the more affordable and efficient scale of autonomous aerial robots. This allows for testing more extreme multifunctional design integration principles than ever considered at full scale before, as the robotics design vignettes exemplify effectively. A theme throughout this review is the consideration of multifunctional structures buildup by smart materials in the context of robotic structures, rather than as a small component of a robot or vehicle. This mindset will result in new materials that are scalable across robots as well as full-scale aerospace applications, rather than highly specialized solutions for specific applications. This is because robotic structures are frequently scalable across disciplines and vehicle sizes. As exemplified by how robotic arms use scales from microscopic surgery in the human body up to space station level maintenance in orbit around the earth. The intrinsic scalability of robotic design principles reduces the research and development effort needed at larger scales and enables focusing resources on adapting them for specific use case constraints as well as large-scale manufacturing.

5.2 Aerospace materials design framework and outlook

A central motivation for the developing multifunctional smart materials for robotic structures is that it increases the operating envelope of future aerial vehicles by making them more adaptable and resilient to unfamiliar scenarios in three categories:

- *Improved performance:* The application of smart materials will enable better sensing, control, and actuation, resulting in higher aircraft performance and maneuverability.
- *Expanded use:* Multifunctional robotic structures enabled by smart materials will be able to perform a larger variety of tasks and missions through their ability to use their structure more effectively for a broader set of functions.
- *Environmental resilience:* robotic structures can perform self-monitoring, enable self-healing, perform multiple functions including passive ones to respond robustly in new and uncertain environments.

It is anticipated that future aerospace vehicles will rely heavily on smart materials [183] (Figure 13.iii). These new vehicles will require materials that do not currently exist at a scale or capability for aerospace implementations. On the other hand, in this review, we demonstrate that these technologies are now emerging in aerial robotics motivated by similar applications. While the current robot design concepts for morphing wings and tails as well as grasping mechanisms represent the first successfully flight-tested aerial robotics demonstrators, they already show how avian design principles work within current autonomous aerial robotics constraints. Further, we reviewed several smart material concepts being tested in subscale prototypes for industrial aerospace platforms. For example, Airbus recently completed wind tunnel testing of an aircraft design with morphing wing surfaces[187]. We observe also that the development and application of smart materials is highly interdisciplinary. As a result, materials scientists and engineers need to work even more closely with roboticists and animal flight researchers as well as mechanical, aerospace, electrical, and software engineers to understand the principles and refine the technologies to take them from concepts to industrial applications. In Figure 14, we briefly summarize the connection between the overall robot design principles with the specific applications of smart materials discussed throughout this work.

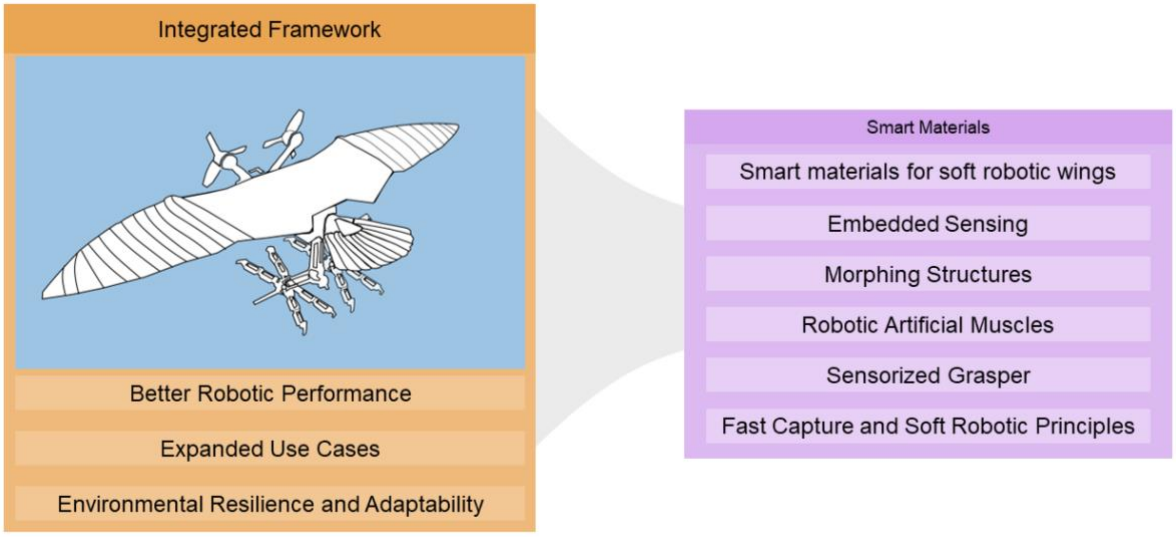

Figure 14 *Summary depicting the relationship between the integrated framework and the smart materials applications discussed throughout this work. The materials in the purple smart materials box will contribute to the various aeras of the integrated framework that will improve overall aerial robot capabilities.*

The last 15 years have seen a proliferation of low-cost and readily available components and open-source software for aerial robots ranging from small quadcopters to large-scale unmanned vehicles. Obtaining and integrating affordable yet highly capable sensors, autopilot systems, compute boards, actuators, and other components using computer-aided manufacturing has never been as easy. The resulted accelerated innovation is unprecedented in industry and research, in education,

and among hobbyist communities[93]. It is now possible to integrate the same sensors used in a guidance system for a helicopter on Mars onto a homemade aerial robot[188]. A similar mindset applied to new smart materials will enable progress in incorporating them into the most capable aerospace platforms. There is therefore a need for the research community to focus on making it easier to discover, understand, procure, integrate, and experiment with multifunctional smart materials in the context of autonomous flight. Such a collective multidisciplinary community approach will help dramatically accelerate the integration of smart materials into aerospace materials and applications.

6 Funding

This research was supported by AFOSR DESI award number FA9550-18-1-0525 with special thanks to B. L. Lee, F. A. Leve, and J. L. Cambier for leading the program. D.L. was also supported by EOARD/IOE grant FA8655 with special thanks to Dr. B. Flake for leading the program. In addition, K.H was supported by an NSF Graduate Research Fellowship and a Stanford Graduate Fellowship, T.G.C was supported by an NSF Graduate Research Fellowship.

1. Chang E, Matloff LY, Stowers AK, et al. Soft biohybrid morphing wings with feathers underactuated by wrist and finger motion. *Sci Robot*; 5. Epub ahead of print 2020. DOI: 10.1126/scirobotics.aay1246.
2. Roderick WRT, Cutkosky MR, Lentink D. Bird-inspired dynamic grasping and perching in arboreal environments. *Sci Robot*; 6. Epub ahead of print 2021. DOI: 10.1126/SCIROBOTICS.ABJ7562.
3. Chen TG, Hoffmann K, Low JE, et al. Aerial Grasping and the Velocity Sufficiency Region. *IROS RAL*.
4. Muijres FT, Johansson LC, Bowlin MS, et al. Comparing aerodynamic efficiency in birds and bats suggests better flight performance in birds. *PLoS One*; 7. Epub ahead of print 2012. DOI: 10.1371/journal.pone.0037335.
5. Tennekes H. The simple science of flight : from insects to jumbo jets, http://site.ebrary.com/id/10331671 (2009).
6. U. M. Norberg. *Vertebrate Flight vol. 27. New York: Springer-Verlag*. 1990.
7. Biewener A, Patek S. *Animal Locomotion*. 2nd ed. Oxford: Oxford University Press. Epub ahead of print 2018. DOI: 10.1093/oso/9780198743156.001.0001.
8. Pennycuick CJ. Chapter 2 The Flight Environment. *Theor Ecol Ser* 2008; 5: 21–36.
9. Videler JJ. Avian flight .
10. Dudley R, Byrnes G, Yanoviak SP, et al. Gliding and the functional origins of flight: Biomechanical novelty or necessity? *Annu Rev Ecol Evol Syst* 2007; 38: 179–201.
11. Mintchev S, Floreano D. Adaptive morphology: A design principle for multimodal and multifunctional robots. *IEEE Robot Autom Mag* 2016; 23: 42–54.
12. Thomas ALR. The flight of birds that have wings and a tail: Variable geometry expands the envelope of flight performance. *J Theor Biol* 1996; 183: 237–245.
13. Cheng B, Tobalske BW, Powers DR, et al. Flight mechanics and control of escape manoeuvres in hummingbirds. I. Flight kinematics. *J Exp Biol* 2016; 219: 3518–3531.
14. Henningsson P, Hedenström A. Aerodynamics of gliding flight in common swifts. *J Exp Biol* 2011; 214: 382–393.
15. Altshuler DL, Bahlman JW, Dakin R, et al. The biophysics of bird flight: Functional relationships integrate aerodynamics, morphology, kinematics, muscles, and sensors. *Can J Zool* 2014; 93: 961–975.
16. Lentink D, Müller UK, Stamhuis EJ, et al. How swifts control their glide performance with morphing wings. *Nature* 2007; 446: 1082–1085.
17. Ortega-Jimenez VM, Sapir N, Wolf M, et al. Into turbulent air: Size-dependent effects of von Kármán vortex streets on hummingbird flight kinematics and energetics. *Proc R Soc B Biol Sci*; 281. Epub ahead of print 2014. DOI: 10.1098/rspb.2014.0180.
18. Ravi S, Crall JD, McNeilly L, et al. Hummingbird flight stability and control in freestream turbulent winds. *J Exp Biol* 2015; 218: 1444–1452.
19. Cheney JA, Stevenson JPJ, Durston NE, et al. Bird wings act as a suspension system that rejects gusts: Bird wings act as a suspension system. *Proc R Soc B Biol Sci*; 287. Epub ahead of print 2020. DOI: 10.1098/rspb.2020.1748rspb20201748.
20. Matloff LY, Chang E, Feo TJ, et al. How flight feathers stick together to form a continuous morphing wing. *Science (80-)* 2020; 367: 293–297.
21. Bachmann T, Emmerlich J, Baumgartner W, et al. Flexural stiffness of feather shafts:

Geometry rules over material properties. *J Exp Biol* 2012; 215: 405–415.
22. Quinn D, Kress D, Chang E, et al. How lovebirds maneuver through lateral gusts with minimal visual information. *Proc Natl Acad Sci U S A* 2019; 116: 15033–15041.
23. Roderick WR, Chin DD, Cutkosky MR, et al. Birds land reliably on complex surfaces by adapting their foot-surface interactions upon contact. *Elife* 2019; 8: 1–23.
24. Brighton CH, Thomas ALR, Taylor GK. Terminal attack trajectories of peregrine falcons are described by the proportional navigation guidance law of missiles. *Proc Natl Acad Sci U S A* 2017; 114: 13495–13500.
25. Chin DD, Matloff LY, Stowers AK, et al. Inspiration for wing design: How forelimb specialization enables active flight in modern vertebrates. *J R Soc Interface*; 14. Epub ahead of print 2017. DOI: 10.1098/rsif.2017.0240.
26. Di Luca M, Mintchev S, Heitz G, et al. Bioinspired morphing wings for extended flight envelope and roll control of small drones. *Interface Focus*; 7, http://rsfs.royalsocietypublishing.org/content/7/1/20160092.abstract (2017).
27. de Croon G. Flapping wing drones show off their skills. *Sci Robot* 2020; 5: 1–3.
28. HAN J, HUI Z, TIAN F, et al. Review on bio-inspired flight systems and bionic aerodynamics. *Chinese J Aeronaut* 2021; 34: 170–186.
29. Lau GK. A stunt flying hawk-inspired drone. *Sci Robot* 2020; 5: 1–3.
30. Katiyar NK, Goel G, Hawi S, et al. Nature-inspired materials: Emerging trends and prospects. *NPG Asia Mater*; 13. Epub ahead of print 2021. DOI: 10.1038/s41427-021-00322-y.
31. McEvoy MA, Correll N. Materials that couple sensing, actuation, computation, and communication. *Science*; 347. Epub ahead of print 2015. DOI: 10.1126/science.1261689.
32. Wang B, Sullivan TN. A review of terrestrial, aerial and aquatic keratins: the structure and mechanical properties of pangolin scales, feather shafts and baleen plates. *J Mech Behav Biomed Mater* 2017; 76: 4–20.
33. Corning WR, Biewener AA. In vivo strains in pigeon flight feather shafts: Implications for structural design. *J Exp Biol* 1998; 201: 3057–3065.
34. Laurent CM, Palmer C, Boardman RP, et al. Nanomechanical properties of bird feather rachises: Exploring naturally occurring fibre reinforced laminar composites. *J R Soc Interface*; 11. Epub ahead of print 2014. DOI: 10.1098/rsif.2014.0961.
35. Galton PM, Shepherd JD. Experimental Analysis of Perching in the European Starling (Sturnus vulgaris: Passeriformes; Passeres), and the Automatic Perching Mechanism of Birds. *J Exp Zool Part A Ecol Genet Physiol* 2012; 317 A: 205–215.
36. Einoder L, Richardson A. An ecomorphological study of the raptorial digital tendon locking mechanism. *Ibis (Lond 1859)* 2006; 148: 515–525.
37. Quinn TH, Baumel JJ. The digital tendon locking mechanism of the avian foot (Aves). *Zoomorphology* 1990; 109: 281–293.
38. Ortega-Jimenez VM, Badger M, Wang H, et al. Into rude air: Hummingbird flight performance in variable aerial environments. *Philos Trans R Soc B Biol Sci*; 371. Epub ahead of print 2016. DOI: 10.1098/rstb.2015.0387.
39. Cheney JA, Stevenson JPJ, Durston NE, et al. Raptor wing morphing with flight speed. *J R Soc Interface*; 18. Epub ahead of print 2021. DOI: 10.1098/rsif.2021.0349.
40. Song J, Cheney JA, Bomphrey RJ, et al. Virtual manipulation of tail postures of a gliding barn owl (Tyto alba) demonstrates drag minimization when gliding. *J R Soc Interface*; 19. Epub ahead of print 2022. DOI: 10.1098/rsif.2021.0710.

41. Dickinson MH, Farley CT, Full RJ, et al. How animals move: An integrative view. *Science (80-)* 2000; 288: 100–106.
42. Ennos A, Hickson J, Roberts A. Functional morphology of the vanes of the flight feathers of the pigeon Columba livia. *J Exp Biol* 1995; 198: 1219–1228.
43. Bachmann T, Klän S, Baumgartner W, et al. Morphometric characterisation of wing feathers of the barn owl Tyto alba pratincola and the pigeon Columba livia. *Front Zool* 2007; 4: 1–15.
44. Hieronymus TL. Flight feather attachment in rock pigeons (Columba livia): covert feathers and smooth muscle coordinate a morphing wing. *J Anat* 2016; 229: 631–656.
45. He B, Wang S, Liu Y. Underactuated robotics: A review. *Int J Adv Robot Syst* 2019; 16: 1–29.
46. Wegst UGK, Ashby MF. The mechanical efficiency of natural materials. *Philos Mag* 2004; 84: 2167–2186.
47. Lazarus BS, Chadha C, Velasco-Hogan A, et al. Engineering with keratin: A functional material and a source of bioinspiration. *iScience* 2021; 24: 102798.
48. Bonser R, Purslow P. The Young's modulus of feather keratin. *J Exp Biol* 1995; 198: 1029–1033.
49. Shyy W, Aono H, Kang C, et al. An Introduction to Flapping Wing Aerodynamics. *An Introd to Flapping Wing Aerodyn*. Epub ahead of print 2013. DOI: 10.1017/cbo9781139583916.
50. Usherwood JR, Hedrick TL, McGowan CP, et al. Dynamic pressure maps for wings and tails of pigeons in slow, flapping flight, and their energetic implications. *J Exp Biol* 2005; 208: 355–369.
51. Dudley R. Mechanisms and implications of animal flight maneuverability. *Integr Comp Biol* 2002; 42: 135–140.
52. Vazquez RJ. The automating skeletal and muscular mechanisms of the avian wing (Aves). *Zoomorphology* 1994; 114: 59–71.
53. Ward AB, Weigl PD, Conroy RM. Functional morphology of raptor hindlimbs: Implications for resource partitioning. *Auk* 2002; 119: 1052–1063.
54. Hudson GE. Studies on the Muscles of the Pelvic Appendage in Birds II: The Heterogeneous Order Falconiformes. *Am Midl Nat* 1948; 39: 102.
55. Brown RE, Fedde MR. Airflow Sensors in the Avian Wing. *J Exp Biol* 1993; 179: 13–30.
56. Maier A. Review article The avian muscle spindle. *Anat Embryol (Berl)* 1992; 186: 1–25.
57. Goldberg JM, Wilson VJ, Cullen KE, et al. *The Vestibular System: A Sixth Sense*. New York: Oxford University Press. Epub ahead of print 2012. DOI: 10.1093/acprof:oso/9780195167085.001.0001.
58. Gibson JJ (James J [author], [provider] T\& FG. *The ecological approach to visual perception*. Classic ed. London ; New York: Routledge, https://www.taylorfrancis.com/books/9781315740218 (2015).
59. Davies M, Green P. *Perception and Motor Control in Birds*. Berlin, Heidelberg: Springer Berlin Heidelberg. Epub ahead of print 1967. DOI: 10.1007/978-3-642-75869-0.
60. Lee DN. General Tau Theory: evolution to date. *Perception* 2009; 38: 837–850.
61. Lee DN, Davies MNO, Green PR, et al. VISUAL CONTROL OF VELOCITY OF APPROACH BY PIGEONS WHEN LANDING. *J Exp Biol* 1993; 180: 85–104.
62. Crandell KE, Smith AF, Crino OL, et al. Coping with compliance during take-off and landing in the diamond dove (Geopelia cuneata). *PLoS One* 2018; 13: 1–14.

63. Burgess S. A review of linkage mechanisms in animal joints and related bioinspired designs. *Bioinspiration and Biomimetics*; 16. Epub ahead of print 2021. DOI: 10.1088/1748-3190/abf744.
64. Lock RJ, Burgess SC, Vaidyanathan R. Multi-modal locomotion: From animal to application. *Bioinspiration and Biomimetics*; 9. Epub ahead of print 2014. DOI: 10.1088/1748-3182/9/1/011001.
65. Stewart W, Ajanic E, Muller M, et al. How to Swoop and Grasp Like a Bird With a Passive Claw for a High-Speed Grasping. *IEEE/ASME Trans Mechatronics* 2022; 1–9.
66. Roderick WRT, Cutkosky MR, Lentink D. Touchdown to take-off: At the interface of flight and surface locomotion. *Interface Focus*; 7. Epub ahead of print 2017. DOI: 10.1098/rsfs.2016.0094.
67. Jeffries L, Lentink D. Design Principles and Function of Mechanical Fasteners in Nature and Technology. *Appl Mech Rev* 2020; 72: 1–24.
68. Li D, Zhao S, Da Ronch A, et al. A review of modelling and analysis of morphing wings. *Prog Aerosp Sci* 2018; 100: 46–62.
69. Jenett B, Calisch S, Cellucci D, et al. Digital Morphing Wing: Active Wing Shaping Concept Using Composite Lattice-Based Cellular Structures. *Soft Robot* 2017; 4: 33–48.
70. Schaedler TA, Jacobsen AJ, Torrents A, et al. Ultralight metallic microlattices. *Science (80-)* 2011; 334: 962–965.
71. Kim D-K, Kang S-G, Park J-Y, et al. Characteristics of piezoresistive mass flow sensor fabricated by porous silicon micromachining. In: *Digest of Papers Microprocesses and Nanotechnology 2000. 2000 International Microprocesses and Nanotechnology Conference (IEEE Cat. No.00EX387)*. 2000, pp. 80–81.
72. Guo Y, Li YH, Guo Z, et al. Bio-inspired stretchable absolute pressure sensor network. *Sensors (Switzerland)* 2016; 16: 1–11.
73. Pak CG. Wing shape sensing from measured strain. *AIAA J* 2016; 54: 1064–1073.
74. Shin H, Ott Z, Beuken LG, et al. Bio-Inspired Large-Area Soft Sensing Skins to Measure UAV Wing Deformation in Flight. 2021; 2100679: 1–12.
75. Xu Y, Jiang F, Newbern S, et al. Flexible shear-stress sensor skin and its application to unmanned aerial vehicles. *Sensors Actuators, A Phys* 2003; 105: 321–329.
76. Mohamed A, Watkins S, Clothier R, et al. Fixed-wing MAV attitude stability in atmospheric turbulence - Part 2: Investigating biologically-inspired sensors. *Prog Aerosp Sci* 2014; 71: 1–13.
77. Lentink D. *Exploring the biofluiddynamics of swimming and flight*, http://library.wur.nl/WebQuery/clc/1894448 (2008).
78. Ajanic E, Feroskhan M, Mintchev S, et al. Bio-Inspired Synergistic Wing and Tail Morphing Extends Flight Capabilities of Drones.
79. Xiong J, Mines R, Ghosh R, et al. Advanced Micro-Lattice Materials. *Adv Eng Mater* 2015; 17: 1253–1264.
80. Wegst UGK, Bai H, Saiz E, et al. Bioinspired structural materials. *Nat Mater* 2015; 14: 23–36.
81. Elliott L V., Salzman EE, Greer JR. Stimuli Responsive Shape Memory Microarchitectures. *Adv Funct Mater* 2021; 31: 1–9.
82. Moestopo WP, Mateos AJ, Fuller RM, et al. Pushing and Pulling on Ropes: Hierarchical Woven Materials. *Adv Sci* 2020; 7: 1–8.
83. Kovač M. The Bioinspiration Design Paradigm: A Perspective for Soft Robotics. *Soft Robot*

2014; 1: 28–37.
84. Raymer DP. *Aircraft design a conceptual approach*. 2018.
85. Stowers AK, Matloff LY, Lentink D. How pigeons couple three-dimensional elbow and wrist motion to morph their wings. *J R Soc Interface*; 14. Epub ahead of print 2017. DOI: 10.1098/rsif.2017.0224.
86. Mao Z, Xu Z, Wang Q. Shape memory alloy actuator with active cooling device and deflectable winglet application. *Smart Mater Struct*; 29. Epub ahead of print 2020. DOI: 10.1088/1361-665X/aba9ab.
87. Han MW, Rodrigue H, Kim H Il, et al. Shape memory alloy/glass fiber woven composite for soft morphing winglets of unmanned aerial vehicles. *Compos Struct* 2016; 140: 202–212.
88. Kota S, Martins JRRA. Flexfloil shape adaptive control surfaces-flight test and numerical results. *31st Congr Int Counc Aeronaut Sci ICAS 2018* 2018; 1–11.
89. Wakayama SR, White E V. Evaluation of Adaptive Compliant Trailing Edge Technology. 2015; 1–12.
90. HAO F, TANG T, GAO Y, et al. Continuous morphing trailing-edge wing concept based on multi-stable nanomaterial. *Chinese J Aeronaut* 2021; 34: 219–231.
91. Cramer NB, Cellucci DW, Formoso OB, et al. Elastic shape morphing of ultralight structures by programmable assembly. *Smart Mater Struct*; 28. Epub ahead of print 2019. DOI: 10.1088/1361-665X/ab0ea2.
92. Xu C, Puente-Santiago AR, Rodríguez-Padrón D, et al. Nature-inspired hierarchical materials for sensing and energy storage applications. *Chem Soc Rev* 2021; 50: 4856–4871.
93. Meier L, Honegger D, Pollefeys M. PX4: A node-based multithreaded open source robotics framework for deeply embedded platforms. *Proc - IEEE Int Conf Robot Autom* 2015; 2015-June: 6235–6240.
94. Mohamed A, Clothier R, Watkins S, et al. Fixed-wing MAV attitude stability in atmospheric turbulence, part 1: Suitability of conventional sensors. *Prog Aerosp Sci* 2014; 70: 69–82.
95. Mohamed A, Massey K, Watkins S, et al. The attitude control of fixed-wing MAVS in turbulent environments. *Prog Aerosp Sci* 2014; 66: 37–48.
96. Huang YA, Zhu C, Xiong WN, et al. Flexible smart sensing skin for "Fly-by-Feel" morphing aircraft. *Science China Technological Sciences* 2022; 65: 1–29.
97. Mohamed A, Watkins S, Fisher A, et al. Bioinspired wing-surface pressure sensing for attitude control of micro air vehicles. *J Aircr* 2015; 52: 827–838.
98. Wood KT, Araujo-Estrada S, Richardson T, et al. Distributed pressure sensing–based flight control for small fixed-wing unmanned aerial systems. *J Aircr* 2019; 56: 1951–1960.
99. Saini A, Gopalarathnam A. Leading-edge flow sensing for aerodynamic parameter estimation. *AIAA J* 2018; 56: 4706–4718.
100. Araujo-Estrada SA, Salama F, Greatwood C, et al. Bio-inspired distributed strain and airflow sensing for small unmanned air vehicle flight control. *AIAA Guid Navig Control Conf 2017*. Epub ahead of print 2017. DOI: 10.2514/6.2017-1487.
101. Fanning JA. In-Flight Measurements Of Freestream Atmospheric Turbulence Intensities.
102. Emmons HW, Bryson AE. The Laminar-Turbulent Transition in a Boundary Layer. *US Natl Congr Theor Appl Mech* 1952; 859–868.
103. Narasimha R. The laminar-turbulent transition zone in the boundary layer. *Prog Aerosp Sci* 1985; 22: 29–80.
104. Anyoji M, Numata D, Nagai H, et al. Pressure-sensitive paint technique for surface pressure

measurements in a low-density wind tunnel. *J Vis* 2015; 18: 297–309.
105. YANG T, ZHONG H, CHEN Y, et al. Transition prediction and sensitivity analysis for a natural laminar flow wing glove flight experiment. *Chinese J Aeronaut* 2021; 34: 34–47.
106. Cox C, Gopalarathnam A, Hall CE. Flight test of stable automated cruise flap for an adaptive wing aircraft. *J Aircr* 2010; 47: 1178–1188.
107. Pinier JT, Ausseur JM, Glauser MN, et al. Proportional closed-loop feedback control of flow separation. *AIAA J* 2007; 45: 181–190.
108. Mohamed A, Abdulrahim M, Watkins S, et al. Development and Flight Testing of a Turbulence Mitigation System for Micro Air Vehicles. *J F Robot* 2016; 33: 639–660.
109. Yeo D, Atkins EM, Bernal LP, et al. Aerodynamic sensing for a fixed wing UAS operating at high angles of attack. *AIAA Atmos Flight Mech Conf 2012*. Epub ahead of print 2012. DOI: 10.2514/6.2012-4416.
110. Jiang F, Xu Y, Weng T, et al. Flexible shear stress sensor skin for aerodynamics applications. *Proc IEEE Micro Electro Mech Syst* 2000; 364–369.
111. Padmanabhan A, Sheplak M, Breuer KS, et al. Micromachined sensors for static and dynamic shear-stress measurements in aerodynamic flows. *Int Conf Solid-State Sensors Actuators, Proc* 1997; 1: 137–140.
112. Barfoot TD. *State Estimation for Robotics*. Cambridge University Press, 2017. Epub ahead of print 2017. DOI: 10.1017/9781316671528.
113. Salowitz N, Guo Z, Kim SJ, et al. Bio-inspired intelligent sensing materials for fly-by-feel autonomous vehicles. *Proc IEEE Sensors* 2012; 1–3.
114. Kopsaftopoulos F, Nardari R, Li YH, et al. A stochastic global identification framework for aerospace structures operating under varying flight states. *Mech Syst Signal Process* 2018; 98: 425–447.
115. Suryakumar VS, Babbar Y, Strganac TW, et al. Control of a Nonlinear Wing Section using Fly-by-Feel. Epub ahead of print 2015. DOI: 10.2514/6.2015-2239.
116. Castano LM, Gremillion GM, Winkelmann AE, et al. Disturbance rejection for an unmanned rotary aircraft system using strain sensing. *J Guid Control Dyn* 2019; 42: 2638–2649.
117. Shi X, Spieler P, Tang E, et al. Adaptive Nonlinear Control of Fixed-Wing VTOL with Airflow Vector Sensing. *Proc - IEEE Int Conf Robot Autom* 2020; 5321–5327.
118. Huang G. Visual-Inertial Navigation : A Concise Review.
119. Bry A. *UNMANNED AERIAL IMAGE CAPTURE PLATFORM*. 10520943, https://patents.google.com/patent/US10520943B2/en (2019).
120. Bachrach A. Skydio Autonomy Engine: Enabling The Next Generation Of Autonomous Flight. In: *2021 IEEE Hot Chips 33 Symposium (HCS)*. IEEE Computer Society, 2021, pp. 1–43.
121. Dasgupta. *Object tracking by an unmanned aerial vehicle using visual sensors*. 2017.
122. Barry AJ, Florence PR, Tedrake R. High-speed autonomous obstacle avoidance with pushbroom stereo. *J F Robot* 2018; 35: 52–68.
123. Mark A, Xu Y, Dickinson BT. Review of microscale flow-sensor-enabled mechanosensing in small unmanned aerial vehicles. *J Aircr* 2019; 56: 962–973.
124. Wallin TJ, Pikul J, Shepherd RF. 3D printing of soft robotic systems. *Nat Rev Mater* 2018; 3: 84–100.
125. Abdulkarem M, Samsudin K, Rokhani FZ, et al. Wireless sensor network for structural health monitoring: A contemporary review of technologies, challenges, and future direction.

Struct Heal Monit 2020; 19: 693–735.
126. Chen X, Topac T, Smith W, et al. Characterization of distributed microfabricated strain gauges on stretchable sensor networks for structural applications. *Sensors (Switzerland)* 2018; 18: 1–14.
127. Lipomi DJ, Vosgueritchian M, Tee BCK, et al. Skin-like pressure and strain sensors based on transparent elastic films of carbon nanotubes. *Nat Nanotechnol* 2011; 6: 788–792.
128. Shih B, Shah D, Li J, et al. Electronic skins and machine learning for intelligent soft robots. *Sci Robot*; 5. Epub ahead of print 2020. DOI: 10.1126/SCIROBOTICS.AAZ9239.
129. Doyle CE, Bird JJ, Isom TA, et al. Avian-inspired passive perching mechanism for robotic rotorcraft. *IEEE Int Conf Intell Robot Syst* 2011; 4975–4980.
130. Kovač M, Germann J, Hürzeler C, et al. A perching mechanism for micro aerial vehicles. *J Micro-Nano Mechatronics* 2009; 5: 77–91.
131. Meng J, Buzzatto J, Liu Y, et al. On Aerial Robots with Grasping and Perching Capabilities: A Comprehensive Review. *Front Robot AI* 2022; 8: 1–24.
132. Hwang D, Barron EJ, Haque ABMT, et al. Shape morphing mechanical metamaterials through reversible plasticity. *Sci Robot* 2022; 7: eabg2171.
133. Falanga D, Kleber K, Mintchev S, et al. The Foldable Drone: A Morphing Quadrotor That Can Squeeze and Fly. *IEEE Robot Autom Lett* 2019; 4: 209–216.
134. Kuder IK, Arrieta AF, Raither WE, et al. Variable stiffness material and structural concepts for morphing applications. *Prog Aerosp Sci* 2013; 63: 33–55.
135. Wang L, Yang Y, Chen Y, et al. Controllable and reversible tuning of material rigidity for robot applications. *Mater Today* 2018; 21: 563–576.
136. Rus D, Tolley MT. Design, fabrication and control of origami robots. *Nat Rev Mater* 2018; 3: 101–112.
137. Rockenbauer* F, Jeger* S, Beltran L, et al. Dipper: A Dynamically Transitioning Aerial-Aquatic Unmanned Vehicle. Epub ahead of print 2021. DOI: 10.15607/rss.2021.xvii.048.
138. SUMPF, JR. RD, PIRES A, STOCKTON WB, et al. *WO2021102340 - INTEGRATED ENERGY STORAGE SYSTEM*. 2021.
139. Ladpli P, Nardari R, Kopsaftopoulos F, et al. Multifunctional energy storage composite structures with embedded lithium-ion batteries. *J Power Sources* 2019; 414: 517–529.
140. Aubin CA, Gorissen B, Milana E, et al. Towards enduring autonomous robots via embodied energy. *Nature* 2022; 602: 393–402.
141. Hassanalian M, Abdelkefi A. Classifications, applications, and design challenges of drones: A review. *Prog Aerosp Sci* 2017; 91: 99–131.
142. Zhang J, Sheng J, O'Neill CT, et al. Robotic Artificial Muscles: Current Progress and Future Perspectives. *IEEE Trans Robot* 2019; 35: 761–781.
143. Acome E, Mitchell SK, Morrissey TG, et al. Hydraulically amplified self-healing electrostatic actuators with muscle-like performance. *Science (80-)* 2018; 359: 61–65.
144. Chen Y, Zhao H, Mao J, et al. Controlled flight of a microrobot powered by soft artificial muscles. *Nature* 2019; 575: 324–329.
145. Nazma E, Mohd S. Tendon Driven Robotic Hands: a Review. *Int J Mech Eng Rob Res Ehtesham Nazma Suhaib Mohd*; 1.
146. Rothemund P, Kellaris N, Mitchell SK, et al. HASEL Artificial Muscles for a New Generation of Lifelike Robots—Recent Progress and Future Opportunities. *Adv Mater* 2021; 33: 1–28.
147. Ren Z, Kim S, Ji X, et al. A High-Lift Micro-Aerial-Robot Powered by Low-Voltage and

Long-Endurance Dielectric Elastomer Actuators. *Adv Mater*; 34. Epub ahead of print 2022. DOI: 10.1002/adma.202106757.
148. Shi M, Yeatman EM. A comparative review of artificial muscles for microsystem applications. *Microsystems Nanoeng*; 7. Epub ahead of print 2021. DOI: 10.1038/s41378-021-00323-5.
149. Safavynia SA, Torres-Oviedo G, Ting LH. Muscle Synergies: Implications for Clinical Evaluation and Rehabilitation of Movement. *Top Spinal Cord Inj Rehabil* 2011; 17: 16–24.
150. Wakeling JM, Lee SSM, Arnold AS, et al. A muscle's force depends on the recruitment patterns of its fibers. *Ann Biomed Eng* 2012; 40: 1708–1720.
151. Wang J, Gao D, Lee PS. Recent Progress in Artificial Muscles for Interactive Soft Robotics. *Adv Mater* 2021; 33: 1–20.
152. Marden JH. Maximum lift production during takeoff in flying animals. *J Exp Biol* 1987; Vol. 130: 235–258.
153. Chi X, Wang S, Zhang Y, et al. A tailless butterfly-type ornithopter with low aspect ratio wings. *IET Conf Publ* 2018; 2018: 4–9.
154. Bullen RD, McKenzie NL. Bat flight-muscle mass: Implications for foraging strategy. *Aust J Zool* 2004; 52: 605–622.
155. Phan HV, Park HC. Insect-inspired, tailless, hover-capable flapping-wing robots: Recent progress, challenges, and future directions. *Prog Aerosp Sci* 2019; 111: 100573.
156. Wells DJ. Muscle Performance in Hovering Hummingbirds. *J Exp Biol* 1993; 178: 39–57.
157. Muijres FT, Elzinga MJ, Melis JM, et al. Flies Evade Looming Targets by Executing Rapid Visually Directed Banked Turns. *Science (80-)* 2014; 344: 172–177.
158. Takahashi H, Abe K, Takahata T, et al. Experimental study of the aerodynamic interaction between the forewing and hindwing of a beetle-type ornithopter. *Aerospace*; 5. Epub ahead of print 2018. DOI: 10.3390/aerospace5030083.
159. Chin YW, Ang Z, Luo Y, et al. Spring-assisted motorized transmission for efficient hover by four flapping wings. *J Mech Robot* 2018; 10: 1–12.
160. Ozaki T, Hamaguchi K. Bioinspired Flapping-Wing Robot with Direct-Driven Piezoelectric Actuation and Its Takeoff Demonstration. *IEEE Robot Autom Lett* 2018; 3: 4217–4224.
161. Decroon GCHE, Perçin M, Remes BDW, et al. *The delfly: Design, aerodynamics, and artificial intelligence of a flapping wing robot*. 2015. Epub ahead of print 2015. DOI: 10.1007/978-94-017-9208-0.
162. Karasek M, Muijres FT, Wagter C De, et al. A tailless aerial robotic flapper reveals that flies use torque coupling in rapid banked turns. *Science (80-)* 2018; 361: 1089–1094.
163. Coleman D, Benedict M. Design , Development and Flight-Testing of a Robotic Hummingbird. *Am Helicopter Soc 71st Annu Forum*.
164. Billard A, Kragic D. Trends and challenges in robot manipulation. *Science (80-)*; 364. Epub ahead of print 2019. DOI: 10.1126/science.aat8414.
165. Chen TG, Hoffmann KAW, Low JE, et al. Aerial Grasping and the Velocity Sufficiency Region. *IEEE Robot Autom Lett* 2022; 7: 10009–10016.
166. Hartman FA. Locomotor Mechanisms. *Smithson Misc Collect*; 143.
167. Markish J. Valuation techniques for commercial aircraft program design. *Massachusetts Inst Technol* 2002; 153.
168. Wang H, Totaro M, Beccai L. Toward Perceptive Soft Robots: Progress and Challenges. *Adv Sci*; 5. Epub ahead of print 2018. DOI: 10.1002/advs.201800541.

169. Bai H, Li S, Barreiros J, et al. Stretchable distributed fiber-optic sensors. *Science (80-)* 2020; 370: 848–852.
170. Liu SQ, Adelson EH. GelSight Fin Ray: Incorporating Tactile Sensing into a Soft Compliant Robotic Gripper, http://arxiv.org/abs/2204.07146 (2022).
171. Shintake J, Cacucciolo V, Floreano D, et al. Soft Robotic Grippers. *Adv Mater*; 30. Epub ahead of print 2018. DOI: 10.1002/adma.201707035.
172. Rajesh RJ, Kavitha P. Camera gimbal stabilization using conventional PID controller and evolutionary algorithms. *IEEE Int Conf Comput Commun Control IC4 2015* 2016; 1–6.
173. Howe RD. Tactile sensing and control of robotic manipulation. *Adv Robot* 1993; 8: 245–261.
174. Kashiri N, Malzahn J, Tsagarakis NG. On the Sensor Design of Torque Controlled Actuators: A Comparison Study of Strain Gauge and Encoder-Based Principles. *IEEE Robot Autom Lett* 2017; 2: 1186–1194.
175. Li S, Bai H, Shepherd RF, et al. Bio-inspired Design and Additive Manufacturing of Soft Materials, Machines, Robots, and Haptic Interfaces. *Angew Chemie - Int Ed* 2019; 58: 11182–11204.
176. Mrad N, Xiao G, Guo H. Micro-size optical fibre strain interrogation system. *Smart Sens Phenomena, Technol Networks, Syst 2008* 2008; 6933: 693304.
177. Mellinger D, Lindsey Q, Shomin M, et al. Design, modeling, estimation and control for aerial grasping and manipulation. *IEEE Int Conf Intell Robot Syst* 2011; 2668–2673.
178. Yuan W, Dong S, Adelson EH. GelSight: High-resolution robot tactile sensors for estimating geometry and force. *Sensors (Switzerland)*; 17. Epub ahead of print 2017. DOI: 10.3390/s17122762.
179. Liu Y, Luo K, Wang S, et al. A Soft and Bistable Gripper with Adjustable Energy Barrier for Fast Capture in Space. *Soft Robot* 2022; 00: 1–11.
180. Brown E, Rodenberg N, Amend J, et al. Universal robotic gripper based on the jamming of granular material. *Proc Natl Acad Sci U S A* 2010; 107: 18809–18814.
181. Phractyl. MACROBAT - Phractyl. 2022.
182. Ai H, Yoshida A, Yokohari F. Vibration receptive sensilla on the wing margins of the silkworm moth Bombyx mori. *J Insect Physiol* 2010; 56: 236–246.
183. Airbus. An Airbus futuristic conceptual airliner “takes flight” to inspire next-generation engineers.
184. Phractyl. MACROBAT - Phractyl. 2022.
185. Hughes D, Correll N. A soft, amorphous skin that can sense and localize textures. *Proc - IEEE Int Conf Robot Autom* 2014; 1844–1851.
186. Karásek M. Flapper Drones, https://flapper-drones.com/wp/.
187. Airbus. Nature-inspired wing demonstrator completes wind-tunnel tests.
188. Bob Balaram J, Canham T, Duncan C, et al. Mars helicopter technology demonstrator. *AIAA Atmos Flight Mech Conf 2018*. Epub ahead of print 2018. DOI: 10.2514/6.2018-0023.